Journal of Medicinal Chemistry

Drug Annotation

Discovery and Synthesis of a Phosphoramidate Prodrug of a Pyrrolo[2,1-*f*][triazin-4-amino] Adenine *C*-Nucleoside (GS-5734) for the Treatment of Ebola and Emerging Viruses

Dustin Siegel, Hon C. Hui, Edward Doerffler, Michael O. Clarke, Kwon Chun, Lijun Zhang, Sean Neville, Ernest Carra, Willard Lew, Bruce Saxby Ross, Queenie Wang, Lydia C. Wolfe, Robert Jordan, Veronica Soloveva, John Edward Knox, Jason Perry, Michel Perron, Kirsten M. Stray, Ona Barauskas, Joy Y. Feng, Yili Xu, Gary Lee, Arnold L. Rheingold, Adrian S. Ray, Roy Bannister, Robert Strickley, Swami Swaminathan, William A. Lee, Sina Bavari, Tomas Cihlar, Michael K. Lo, Travis K. Warren, and Richard L. Mackman

J. Med. Chem., **Just Accepted Manuscript** • Publication Date (Web): 26 Jan 2017

Just Accepted

Discovery and Synthesis of a Phosphoramidate Prodrug of a Pyrrolo[2,1-*f*][triazin-4-amino] Adenine *C*-Nucleoside (GS-5734) for the Treatment of Ebola and Emerging Viruses

Dustin Siegel[1], Hon C. Hui[1], Edward Doerffler[1], Michael O. Clarke[1], Kwon Chun[1], Lijun Zhang[1], Sean Neville[1], Ernest Carra[1], Willard Lew[1], Bruce Ross[1], Queenie Wang[1], Lydia Wolfe[1], Robert Jordan[1], Veronica Soloveva[2], John Knox[1], Jason Perry[1], Michel Perron[1], Kirsten M. Stray[1], Ona Barauskas[1], Joy Y. Feng[1], Yili Xu[1], Gary Lee[1], Arnold L. Rheingold[3], Adrian S. Ray[1], Roy Bannister[1], Robert Strickley[1], Swami Swaminathan[1], William A. Lee[1], Sina Bavari[2], Tomas Cihlar[1], Michael K. Lo[4], Travis K. Warren[2], and Richard L. Mackman[1]*

[1]Gilead Sciences, Inc., Foster City, California, USA.

[2]United States Army Medical Research Institute of Infectious Diseases (USAMRIID), Frederick, Maryland, USA.

[3]UC San Diego, San Diego, California, USA.

[4]Centers for Disease Control and Prevention, Atlanta, Georgia, USA.

ABSTRACT

The recent Ebola Virus (EBOV) outbreak in West Africa was the largest recorded in history with over 28,000 cases, resulting in >11,000 deaths including >500 healthcare workers. A focused screening and lead optimization effort identified **4b** (GS-5734) with anti-EBOV EC_{50}=86 nM in macrophages as the clinical candidate. Structure activity relationships established that the 1′-CN group and *C*-linked nucleobase were critical for optimal anti-EBOV potency and selectivity against host polymerases. A robust diastereoselective synthesis provided sufficient quantities of **4b** to enable preclinical efficacy in a nonhuman primate EBOV challenge model. Once-daily 10 mg/kg iv treatment on days 3-14 post infection had a significant effect on viremia and mortality, resulting in 100% survival of infected treated animals [*Nature* **2016**, *531*, 381-385]. A phase 2 study (PREVAIL IV) is currently enrolling and will evaluate the effect of **4b** on viral shedding from sanctuary sites in EBOV survivors.

INTRODUCTION

Ebola Virus Disease (EVD) was first documented 40 years ago during an outbreak of infectious hemorrhagic fever in Northern Zaire (current Democratic Republic of Congo). More than 20 intermittent outbreaks have occurred since then, but the most recent outbreak in West Africa spanning 2013-2016 has been the largest recorded in history and presented an international public health emergency.[1] Over 28,000 cases were confirmed in Guinea, Liberia, and Sierra Leone resulting in >11,000 deaths including >500 healthcare workers, which severely strained the local medical infrastructure.[2] In survivors, the Ebola virus (EBOV) can persist in bodily fluids for months after the onset of acute infection potentially leading to EVD-related sequelae and viral recrudescence.[3] While rare, secondary transmission has been documented to occur through sexual intercourse implicating persistent virus in genital secretions.[4] Despite the end of the current outbreak, the potential for equally devastating future outbreaks together with the persistent virus observed in survivors makes the development of a safe, effective and readily available treatment option for EVD a high priority.

EBOV, a member of the *Filoviridae* family, is a single-stranded, negative-sense, non-segmented RNA virus that is the causative agent of EVD. Other *Filoviridae* family members include Marburg, Sudan, and Bundibugyo viruses, which have all been responsible for outbreaks associated with high mortality rates in sub-Saharan Africa.[5,6] Over the course of the recent West African EVD outbreak, several direct acting anti-Ebola agents including monoclonal antibodies (ZMapp™),[7] interfering-RNAs[8-10], and small molecule nucleoside(tide) antivirals such as favipiravir (**1**),[11-13] and brincidofovir (**2**)[14] have been evaluated in early clinical trials (Figure 1). More recently another nucleoside analogue, galidesivir (**3**, BCX4430[15]), has entered clinical development. These developments are encouraging but to date, none of these potential

therapeutics have established robust clinical efficacy for the treatment of acute infection or the viral persistence and sequelae. Several vaccines have shown strong promise for preventing EBOV infection, but the breadth and durability of protection they can afford has yet to be established.[16]

Figure 1. Structures of antiviral nucleosides and nucleoside phosphonates.

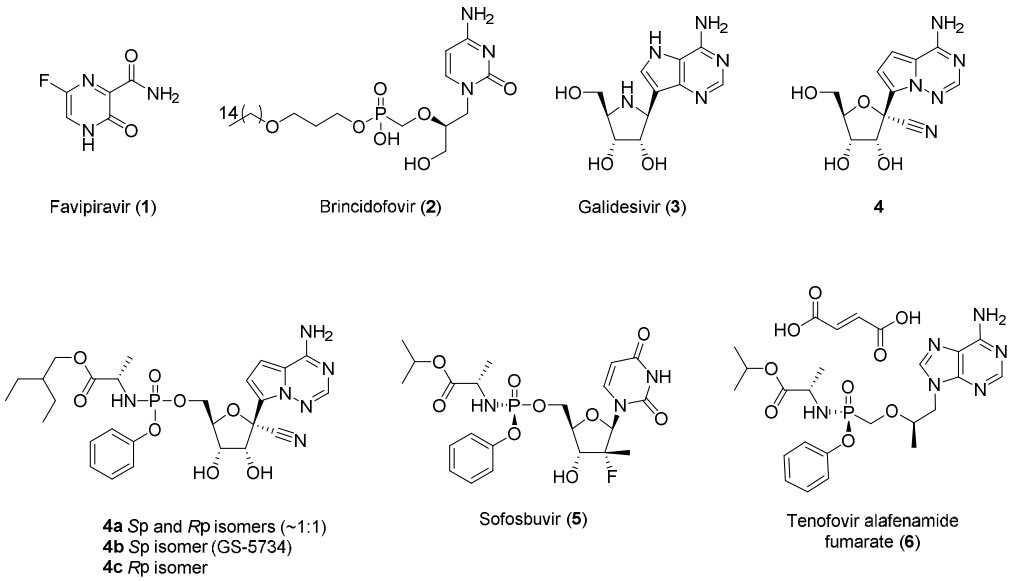

Prior to the Ebola outbreak, we had embarked on a strategic initiative aimed at evaluating the potential of nucleoside analogs for the treatment of selected emerging viruses. A library of ~ 1000 diverse nucleoside and nucleoside phosphonate analogs was harnessed from over two decades of research across multiple antiviral programs. In collaboration with the Center for Disease Control and Prevention (CDC), and the United States Army Medical Research Institute of Infectious Diseases (USAMRIID), selected compounds from the library were screened against EBOV, leading to the identification of parent **4** and a potent monophosphate prodrug mixture **4a** that contained the single *S*p isomer **4b** (GS-5734[17]) that was selected for development. This

report describes in detail the structure activity relationships (SAR) of the parent nucleoside, prodrug optimization and selection, and synthesis optimization of the development candidate **4b**. Candidate compound **4b** is currently in phase 2 trials to assess the effect on the chronic shedding of virus in EVD survivors following promising efficacy data established in a nonhuman primate (NHP) EVD challenge model. These data have been recently reported[17] and will be summarized along with the early clinical experience with **4b**.

RESULTS AND DISCUSSION

The assembly of the ~1000 compound nucleos(t)ide screening library was heavily focused toward ribose analogs that could target RNA viruses since this would encompass many emerging viral infections ranging from respiratory pathogens belonging to the *coronaviridae* family such as severe acute respiratory syndrome (SARS) and Middle East respiratory syndrome (MERS), to mosquito-borne viruses of the *flaviviridae* family such as Dengue and Zika. The majority of the library compounds were nucleosides that contained a cyclic modified ribose or 'ribose-like' core. These nucleosides were also predominantly *N*-nucleosides. Less than 10% of the library comprised nucleoside phosphonates or acyclic analogs due to the limited success, to date, in identifying potent RNA virus inhibitors with these types of analogs. A second key factor in the library assembly was that approximately 50% of the library included monophosphate and ester prodrugs to capture analogs that may be missed in cellular screens due to either poor permeability or inefficient metabolism in the respective cell types that the different antiviral assays utilize. Nucleoside analogs require activation by intracellular nucleoside/tide kinases to generate their respective nucleoside triphosphate (NTP) metabolites in order to then compete with endogenous natural nucleotide pools for incorporation into the replicating viral RNA.[17] The

first phosphorylation step to generate the nucleoside monophosphate is often rate limiting and therefore the application of monophosphate prodrugs, especially phosphoramidates (ProTides™), has been extensively explored in nucleoside analogs to bypass this initial phosphorylation step.[18] A notable example includes the phosphoramidate prodrug Sofosbuvir (**5**) for the treatment of HCV (Figure 1).[19] Nucleoside phosphonate analogs are bioisosteres of the monophosphates but also require prodrugs to enable masking of the charged phosphonate acid thereby allowing more efficient entry into cells. A recent example of an approved drug in this class is the phosphonamidate prodrug tenofovir alafenamide (**6**) for the treatment of HIV.[20] In both examples the amidate prodrugs effectively deliver high levels of triphosphate (diphosphophosphonate in the case of nucleoside phosphonates) inside the target cells and demonstrate significant improvements in potency compared to their respective parent nucleos(t)ides when screened in antiviral assays.[20,21]

In the original library screening toward a panel of RNA viruses across different viral families, promising leads were identified. Subsequent to the EVD outbreak, some of these analogs were selected for EBOV testing in collaboration with the CDC and USAMRIID in a BSL-4 facility. From this screen nucleoside **4**[22], a 1′-CN modified adenosine *C*-nucleoside emerged with submicromolar activity towards EBOV in Human Microvascular Endothelial Cells (HMVEC-TERT) cells (entry 2, Table 1). In addition, its phosphoramidate prodrug mixture **4a**[23] (entry 3, Table 1) containing ~1:1 ratio of *S*p **4b** and *R*p **4c** diastereoisomers (Figure 1) was found to be very potent toward EBOV in both HeLa and HMVEC cells. Encouraged by these data, the anti-EBOV activity for a range of nucleoside analogs and their prodrugs was evaluated and the results are reported in Table 1, along with activity toward respiratory syncytial virus (RSV), from the *pneumoviridae* family, and HCV, from the *flaviviridae* family.

Table 1. SAR of nucleoside parents and selected prodrugs.[1]

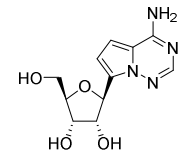

7

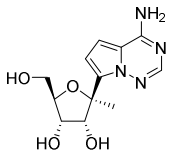

8

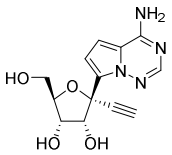

9

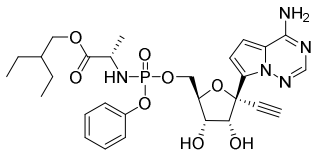

9a

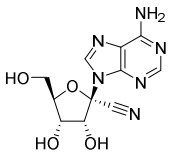

10

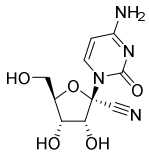

11

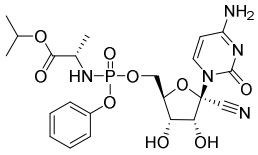

11a

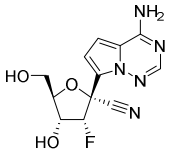

12

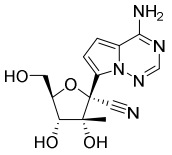

13

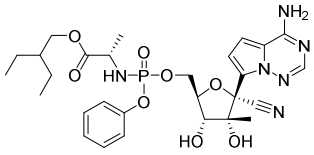

13a

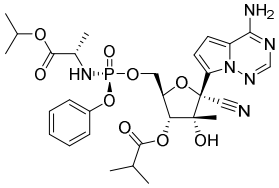

13b

Entry	Compound	EBOV EC_{50} HeLa cells (μM)	EBOV EC_{50} HMVEC cells[2] (μM)	RSV EC_{50} HEp-2 cells (μM)	HCV 1b EC_{50} Huh-7 cells (μM)	CC_{50} HEp-2 cells (μM)	CC_{50} Huh-7 cells (μM)	CC_{50} MT4 cells (μM)
1	**7**	--	--	--	0.0035	0.038[3]	0.15	<0.01
2	**4**	>20	0.78	0.53	4.1	>100	>88	>57
3	**4a**	0.17	0.12	0.027	0.023[4]	9.2	17[4]	2.0
4	**4b**	0.10	0.053	0.015	0.057	6.1	36	1.7
5	**8**	--	>10	5.5	38	93	62	4.5
6	**9**	--	--	>200	>88	>200	>88	120
7	**9a**	--	3.9	1.1	6.9	>100	>44	>32
8	**10**	--	56	>100	>44	>100	>88	>53
9	**11**	>50	>10	7.3	12	>100	>44	>57
10	**11a**	>20	--	63	2.5	>100	>44	53
11	**12**	--	--	>100[3]	>44	--	>44	32[3]
12	**13**	50	>10	>100	>44	>100	>44	>57
13	**13a**	27	13[4]	>50	0.37	>50	>44	1.4
14	**13b**	>20	40	>20	0.31	95	51	7.8

[1]Data reported is at least n≥2 in 384 well assay format unless otherwise noted. [2]HMVEC cells = TERT-immortalized human foreskin microvascular endothelial cells (ATCC-4025) cells. [3]96 well assay format. [4]n=1 data only.

The presence of the 1′-CN modification in **4** was found to be critical in providing selectivity toward viral polymerases and avoiding the significant toxicity (CC_{50}<0.01 – 0.15 μM) associated with the unmodified *C*-nucleoside **7** (entry 1, Table 1).[24] The MT4 cell line was also used as a sensitive cell line to evaluate cytostatic effects of nucleoside analogs, and confirmed the poor selectivity of **7** observed in both the HEp-2 and Huh-7 cell lines. The prodrug mixture **4a** in addition to potent anti-EBOV activity, demonstrated significant activity toward RSV and HCV, with potencies similar or better than that for EBOV (EC_{50}<120 nM). The broad and potent antiviral activity across all three viruses for **4a** was further supported by the potent activity of the single *S*p isomer **4b** toward the same viruses and also other emerging RNA viruses such as MERS and Junin viruses, and to a lesser extent Lassa.[17] The antiviral selectivity of **4b** toward EBOV was 17-32 fold compared to the MT4 cell line CC_{50}, and higher in the other cell types reported in Table 1. Given the anticipated short treatment duration for EVD, this window of in vitro selectivity was considered sufficient for continued interest in **4b**. The 1′-methyl analog **8** (entry 5)[22] was less active toward EBOV and also displayed a higher degree of toxicity compared to the 1′-CN analog **4** illustrating how small changes in the polarity and size of the 1′ substituent can impact the overall profile. The 1′-ethynyl analog **9** (entry 6)[22] and its corresponding 2-ethylbutyl alanine prodrug **9a** (entry 7) were both less active when compared to their respective 1′-CN counterparts (**4** and **4a** respectively).

Compound **4** is a *C*-nucleoside analog which provides chemical and enzymatic stability toward deglycosylation reactions at the anomeric center. However, alternate base modifications including *N*-nucleosides were also studied. Interestingly, the corresponding 1′-CN modified adenosine *N*-analog **10** (entry 8)[25] was significantly less active toward all viruses, whilst the 1′-CN modified *N*-nucleoside pyrimidine **11** (entry 9) retained weak antiviral activity only for RSV

and HCV.[26,27] The phosphoramidate prodrug of 1′-CN cytidine **11a** (entry 10)[27] did not improve the potency toward EBOV (in HeLa cell assay) or the other viruses tested, presumably due to limitations in metabolism beyond the monophosphate. In general, the potency trends of 1′ substitution and nucleobase changes were similar across EBOV, RSV and HCV, which was in contrast to the trends uncovered with 2′ modifications. The 2′-deoxy-2′-fluorine analog **12** (entry 11)[23] and the 2′-β-methyl analog **13** (entry 12)[28] both lacked significant antiviral activity. However, the 2′-β-methyl phosphoramidate prodrugs, analogs **13a** and **13b** (entries 13 and 14)[28] respectively, were both potent toward HCV, and only weakly active/inactive toward EBOV and RSV. This result suggests that HCV polymerase is more able to accommodate the 2′-β-methyl group compared to the EBOV and RSV polymerases. Taken together with the 1′ substitution and nucleobase SAR, the EBOV and RSV polymerases demonstrated similar activity trends, whilst HCV polymerase was differentiated in SAR at the 2′ position.

To interrogate the cell based SAR more rigorously the active NTP metabolite **4tp**[23] was tested toward the viral polymerases (Table 2). The triphosphate **4tp** demonstrated a half-maximal inhibitory concentration (IC_{50}) of 1.1 μM against the RSV RdRp and 5.0 μM against HCV RdRp. The Ebola viral polymerase has to date evaded efforts toward its isolation and expression so the intrinsic activity of the active NTP metabolite cannot be directly evaluated. An alternate method for estimating the inhibitory properties of an NTP for its viral target is to measure the NTP levels inside cells following incubation with the parent or prodrug compound at a given concentration, and then calculate the NTP levels at the EC_{50} measured in the same cells.[17] For example, in a continuous 72 h incubation of 1 μM **4a**, the **4tp** levels were measured at 2, 24, 48 and 72 h, and reached a C_{max} of 300, 110, and 90 pmol/million cells in macrophages, HMVEC, and HeLa cells lines respectively. The several fold difference in maximum NTP levels is not

unusual and reflects the differences between cells with respect to their ability to break down the prodrug and subsequently metabolize the released monophosphate to the active NTP. The average NTP levels over the 72 h incubation of **4a** were then used along with an average cell volume of 2 pL[29] to calculate an estimated half-maximal inhibitory concentration of ~5 μM for the intracellular inhibition of EBOV polymerase. This is comparable in potency toward RSV and HCV polymerases supporting the potent antiviral EC_{50} data demonstrated for the prodrug mixture **4a** across the three viruses when allowing for cell differences (Table 1). The selective inhibition of the viral polymerases versus host polymerases is considered a key factor in the development of a safe and effective nucleoside antiviral.[30,31] Therefore **4tp** was evaluated toward several host polymerases and was found to be a weak incorporator toward mitochondrial polymerase (POLRMT), and not a substrate for DNA polymerase γ, as would be expected given the presence of the ribose 2′ OH (Table 2). Across the host RNA and DNA polymerases evaluated there was no inhibition up to 200 μM (Table 2) demonstrating a high degree of selectivity of **4tp** toward the viral polymerases compared to representative examples of host polymerases.

Table 2. Inhibition of RSV polymerase, HCV polymerase, and human polymerases by 4tp.

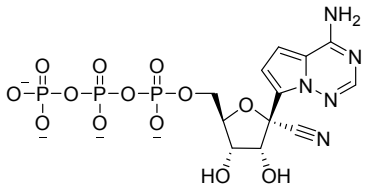

4tp

Enzyme	4tp IC_{50} (μM)	4tp SNI[1] rate (%)
RSV RdRp	1.1	-
HCV RdRp	5	-

POLRMT	>200	6
RNA Pol II	>200	-
DNA Pol α	>200	-
DNA Pol β	>200	-
DNA Pol γ	>200	0

[1]SNI = Single Nucleotide Incorporation

Molecular structure information is not available for the EBOV or RSV polymerases so modeling of the active sites was performed based on the published structures for HIV and HCV polymerases, together with an analysis of the respective sequences.[32] Within the modeled active site of EBOV polymerase the major difference between EBOV and RSV is Y636 (EBOV) compared to F704 (RSV) and the major difference between EBOV and HCV is E709 (EBOV) compared to S282 (HCV). On docking the triphosphate **4tp**, the 1′-CN group occupies a pocket formed by residues that are identical between EBOV and RSV, yet very different in HCV (Figure 2a). Nevertheless the 1′-CN analog retains antiviral potency across these viruses and others[17] suggesting that a pocket exists to accommodate the 1′-CN group in many viral polymerases including other filovirus.[33] The 2′-β-H of **4tp** is in close proximity to E709 and replacement of this group with a 2′-β-methyl (**13tp**) would be anticipated to interfere with E709 (Figure 2b).[34] However, the 2′-β-methyl can be accommodated by the larger pocket afforded by the smaller S282 residue of HCV (Figure 2c). This suggests the lack of activity for 2′-β-methyl analogs toward EBOV and RSV and retained potency toward HCV is likely due to steric constraints in the polymerase active site. Consistent with the model, EBOV and RSV both have the E709 or equivalent residue, and **13tp** was found to be significantly less active (IC_{50}>30 μM) toward RSV.

Figure 2. (a) Compound **4tp** modeled into EBOV polymerase active site. Residue Y636 is highlighted in green surface, sits below the ribose, and corresponds to F704 in RSV. Residue E709 is highlighted in red surface, sits in proximity to the 2′-β-H position of the ribose, and corresponds to S282 in HCV; (b) Compound **13tp** modeled into the EBOV polymerase active site. The 2′-β-methyl overlaps with residue E709 highlighted in red. (c) Compound **13tp** modeled into the HCV polymerase active site. Residue S282 is highlighted in the yellow surface and the 2′-β-methyl can be accommodated.

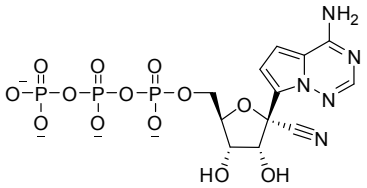

4tp

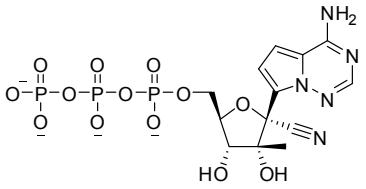

13tp

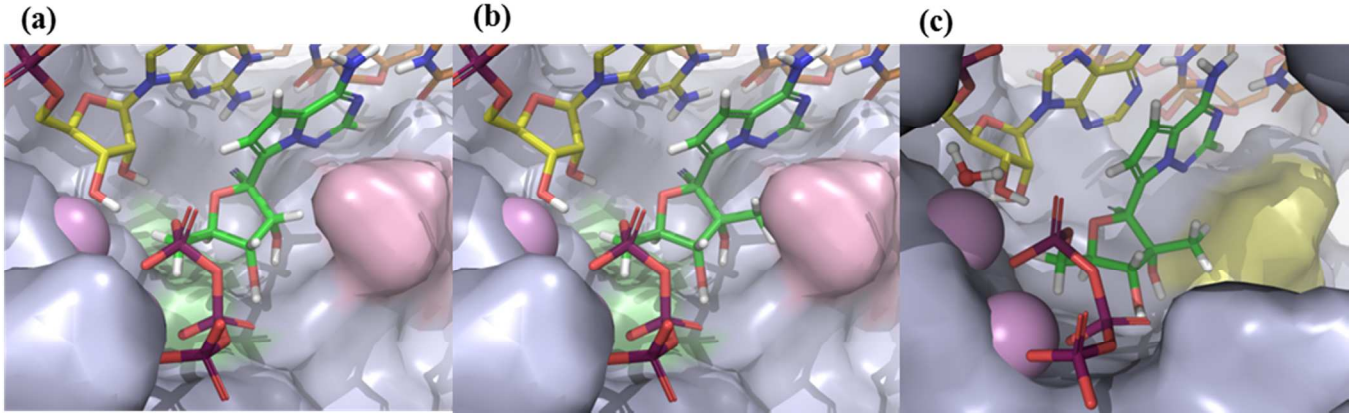

The screening and modeling efforts established **4** as the best lead for prodrug optimization. The ability to evaluate prodrugs, especially in vivo, required an efficient synthesis route for both the nucleoside **4** and preferably, a single prodrug diastereoisomer. Neither was available at the outset so significant chemistry resources were applied to improve the robustness and scalability of the route along with generation of single diastereoisomers. The first generation synthesis of **4** and the single *S*p phosphoramidate prodrug **4b** commenced with a glycosylation reaction via metal-halogen exchange of the bromo-base **15** followed by addition into the

ribolactone **14** (Scheme 1). Two conditions were identified to render this desired C-C bond formation. The first condition (a) proceeded through addition of excess *n*-BuLi to a mixture of TMSCl and **15**, which was designed to result in lithium-halogen exchange after removal of the acidic 6N protons by silyl protection. Addition of this in situ generated reagent to the ribolactone **14** then afforded **16** in 25% yield.[23,35,36] The alternative conditions (b) employed sodium hydride and 1,2-bis(chlorodimethylsilyl)ethane for the 6N protection step, followed by lithium-halogen exchange, and addition to the lactone to afford **16** in 60% yield.[22,36]

Scheme 1. First generation synthesis of **4a**.[a]

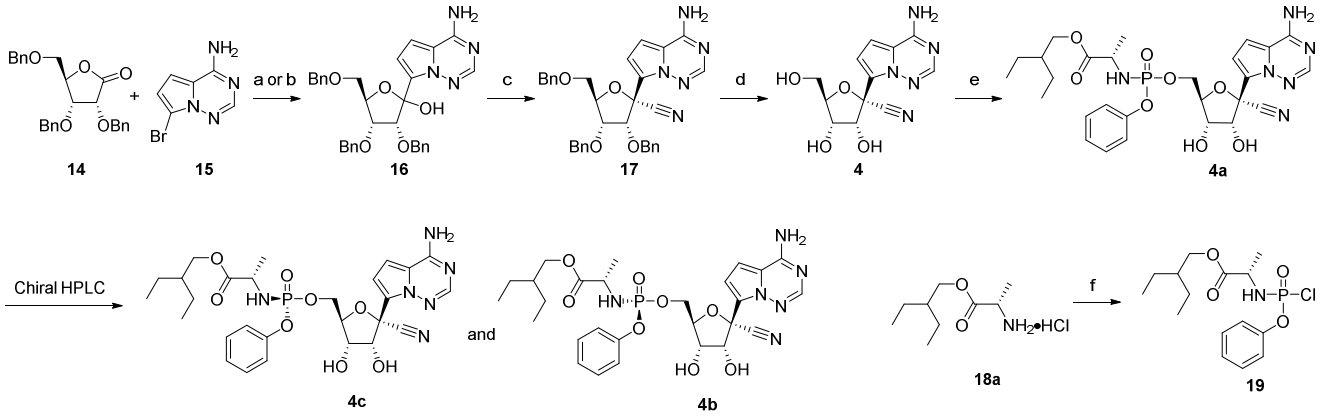

[a]Reagents and conditions: (a) *n*-BuLi, TMSCl, THF, −78 °C, 25%; (b) 1,2-bis(chlorodimethylsilyl)ethane, NaH, *n*-BuLi, THF, −78 °C, 60%; (c) TMSCN, BF_3•Et_2O, CH_2Cl_2, −78 °C, 58% (89:11β-**17**/α). (d) BCl_3, CH_2Cl_2, −78 °C, 74%. (e) **19**, NMI, $OP(OMe)_3$, 21%; (f) $OP(OPh)Cl_2$, Et_3N, CH_2Cl_2, 0 °C, 23%.

The efficiency of both conditions was suboptimal as the yields were capricious and highly dependent on the cryogenic temperatures and the rate of *n*-BuLi addition required for the transformation. Furthermore, premature quenching and reduction of lithio base was observed, which was rationalized to be a consequence of deprotonation alpha to the lactone under the

highly basic conditions. Compound **16** was isolated as a mixture of 1′-isomers, which were taken into the subsequent 1′-cyanation reaction to isolate the major product, β-anomer **17**, by chromatography.[37] Following removal of the three benzyl protecting groups to afford **4**, the diastereomeric mixture of the phosphoramidoyl chloridate prodrug moiety **19**, was then coupled to provide **4a** in 21% yield, as an ~1:1 diastereomeric mixture.[23] The two diastereomers were resolved using chiral HPLC to afford the *S*p isomer **4b** and *R*p isomer **4c** respectively.[38] While this route initially provided quantities of **4b** the variability in yields, suboptimal selectivity, frequent use of cryogenic temperatures, and chiral chromatography, hindered this route from being suited to larger scales.

Scheme 2. Second generation synthesis of **4b**.[a]

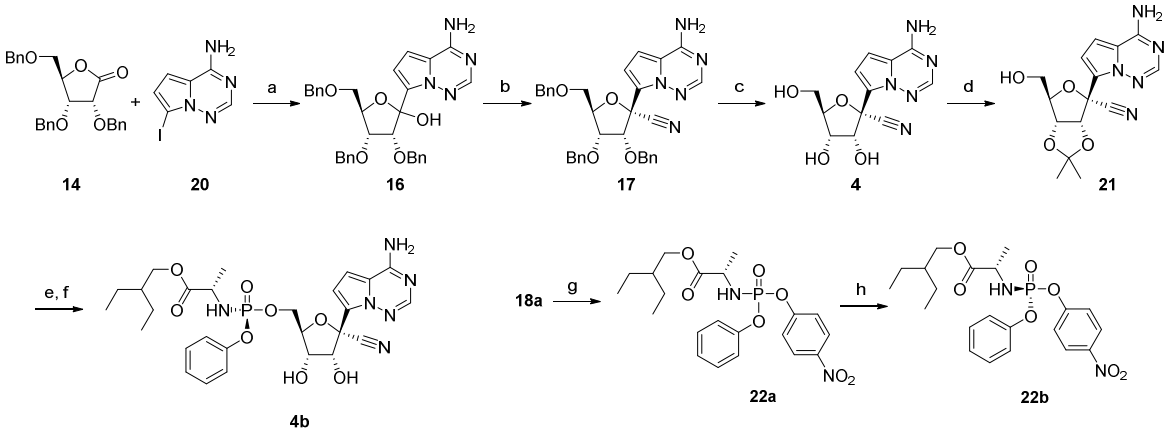

[a]Reagents and conditions: (a) TMSCl, PhMgCl, *i*-PrMgCl•LiCl, THF, −20 °C, 40%; (b) TMSCN, TfOH, TMSOTf, CH_2Cl_2, −78 °C, 85%; (c) BCl_3, CH_2Cl_2, −20 °C, 86%; (d) 2,2-dimethoxypropane, H_2SO_4, acetone, rt, 90%; (e) **22b**, $MgCl_2$, $(i\text{-Pr})_2NEt$, MeCN, 50 °C, 70%; (f) 37% HCl, THF, rt, 69%. (g) $OP(OPh)Cl_2$, Et_3N, CH_2Cl_2, −78 °C, then 4-nitrophenol, Et_3N, 0 °C, 80%; (h) $i\text{-Pr}_2O$, 39%.

The second generation route enabled the diastereoselective synthesis of the single *S*p isomer **4b** on scales suitable to advance the compound into preclinical efficacy and toxicity

studies (Scheme 2).[17] The glycosylation step employed the iodo-base **20** instead of the bromo base which enabled a more facile metal-halogen exchange compatible with *i*-PrMgCl•LiCl complex.[39] Treatment with PhMgCl and TMSCl provided 6N protection to remove the acidic protons with a higher degree of control, and addition of *i*-PrMgCl•LiCl followed by the ribolactone **14** at −20 °C afforded the glycosylation product **16** in a 40% yield. The milder reagents and temperature enabled large-scale batches to be carried out with consistent yields. Treatment of **16** with TMSCN, TMSOTf, and TfOH at −78 °C afforded **17** in 85% yield in >95:5 anomeric ratio. The inclusion of TfOH was key to promote the high yield and high selectivity favoring the desired β-anomer. Benzyl deprotection was effected through treatment with BCl_3 and **4** was readily isolated through crystallization. Acetonide protection of the 2′,3′-hydroxyl moeities with 2,2-dimethoxypropane in the presence of H_2SO_4 afforded **21** in 90% yield. Utilizing the 2′,3′-acetonide protection was found to be optimal as the yield of the coupling reaction with the *p*-nitrophenolate 2-ethylbutyl-L-alaninate prodrug mixture **22a** was dramatically improved compared to directly coupling to the unprotected nucleoside **4** (70% vs 40%). In the event, reaction of **21** with the single *S*p isomer of the *p*-nitrophenolate prodrug precursor **22b** in the presence of $MgCl_2$ and Hunig's base efficiently appended the prodrug group in 70% yield as a single *S*p isomer. Final deprotection of the acetonide with concentrated HCl in THF afforded **4b** in 69% yield.

The single *S*p isomer **22b** of the *p*-nitrophenolate 2-ethylbutyl-L-alaninate prodrug precursor **22a** was prepared through a sequence beginning with exposure of 2-ethylbutyl-L-alanine **18a** to $OP(OPh)Cl_2$, followed by 4-nitrophenol, to afford **22a** as a diastereomeric mixture at phosphorus. Importantly, the single *S*p isomer **22b** was readily resolved from the mixture in 39% yield through crystallization in diisopropyl ether, a discovery that was paramount for the

success of the diastereoselective synthesis of the **4b**.[40] Thus, utilizing the *p*-nitrophenolate 2-ethylbutyl-L-alaninate prodrug coupling partner **22b** offered a significant advantage over the chloridate **19** in the first generation sequence. Overall the second generation synthesis of **4b** offered the following improvements: (1) milder glycosylation conditions at higher temperature to allow for consistent yields and scalability, (2) higher selectivity and yield for the 1′-cyanation reaction, and (3) a highly efficient coupling sequence of a single *S*p prodrug moiety for the diastereoselective synthesis of **4b**. Through this second generation route >200g was rapidly prepared to support preclinical efficacy and toxicity studies.

The stereochemistry of the *p*-nitrophenolate 2-ethylbutyl-L-alaninate prodrug **22b** and candidate compound **4b** were unambiguously assigned by small molecule X-Ray crystallography (Figure 3). In both cases the *S*p isomer was established and suggests that the coupling with the nucleoside and reagent follows a S_N2 type inversion of the phosphorus stereocenter.

Figure 3. Thermal ellipsoid representations of (a) **22b** and (b) **4b**.

(a)

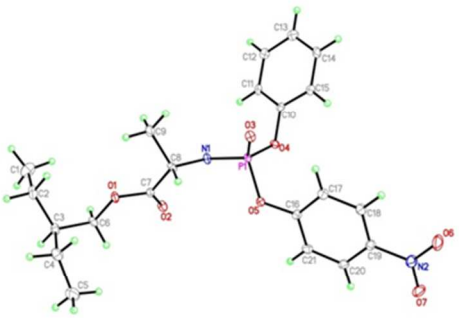

(b)

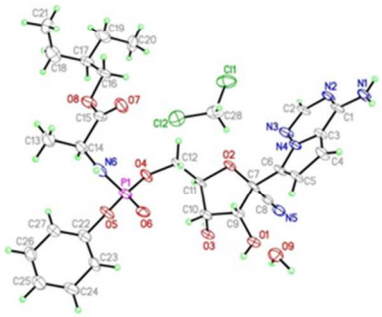

The improved method for preparing **4** enabled many monophosphoramidate and bisphosphoramide prodrug analogues to be synthesized, the results of which are summarized in Scheme 3. A number of conditions were identified to affect the coupling of the prodrug moieties to **4** or the 2′,3′-acetonide protected analogue **21**. The reactions employing **4** proceeded under either Brønsted basic conditions utilizing *t*-BuMgCl or Lewis acidic conditions with $MgCl_2$ in polar aprotic solvents to afford the desired prodrugs in yields ranging from 10-43%. The coupling reaction of the 2′,3′-acetonide protected analogue **21** under lewis acidic conditions followed by in-situ acetonide deprotection in general afforded much higher yields ranging from 60-70% (analogue **4b** and **4n**). Both the *para*-nitrophenol (PNP) and penta-fluorophenol (PFP) prodrug electrophiles were compatible in the coupling reactions and typically achieved comparable yields. The reactions utilizing diastereomeric mixtures of the prodrug electrophiles, **22a**, **d-h**, **j**, **l**, **n** provided the prodrug products in 1.5-2.6 to 1 diastereomeric ratios (unassigned)

at phosphorus. In addition to the monophosphoramidate prodrugs, two bisphosphoramide prodrugs **4o** and **4p** were synthesized and evaluated since they avoided the preparation of chiral phosphorus reagents.

Scheme 3. Prodrug Synthesis.

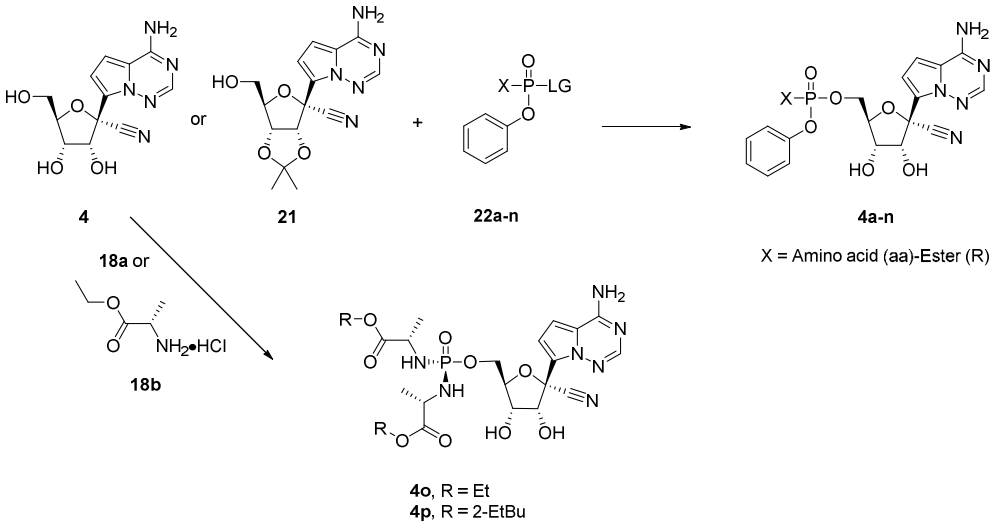

Prodrug[1]	X		LG[3]	Coupling Partner	Conditions	Product	Yield	Isomer Ratio
	Ester R	aa[2]						
22a	2-EtBu	L-Ala	PNP	**4**	*t*-BuMgCl, THF, DMF, rt	**4a**	43%	2.5 : 1
22b[4]	2-EtBu	L-Ala	PNP	**21**	$MgCl_2$, $(i\text{-Pr})_2NEt$, THF, 50 °C; conc. HCl, 0 °C	**4b**	69%	*Sp* Isomer
22d	Et	L-Phe	PNP	**4**	*t*-BuMgCl, THF, DMF, rt	**4d**	34%	2.6 : 1
22e	Et	L-Val	PNP	**4**	*t*-BuMgCl, THF, NMP, rt	**4e**	43%	1.8 : 1
22f	Et	AIB	PNP	**4**	*t*-BuMgCl, THF, NMP, 50 °C	**4f**	25%	1.5 : 1
22g	Et	L-Ala	PNP	**4**	*t*-BuMgCl, THF, NMP, rt	**4g**	24%	2.5 :1
22h	*c*-Bu	L-Ala	PNP	**4**	$MgCl_2$, $(i\text{-Pr})_2NEt$, DMF, 50 °C	**4h**	37%	3 : 2
22i[4]	*i*-Pr	L-Ala	PNP	**4**	*t*-BuMgCl, THF, NMP, 50 °C	**4i**	38%	*Sp* Isomer
22j	*t*-Bu	L-Ala	PNP	**4**	$MgCl_2$, $(i\text{-Pr})_2NEt$, DMF, 50 °C	**4j**	32%	1.5 : 1
22k[5]	*c*-Pent	L-Ala	PFP	**4**	*t*-BuMgCl, THF, DMF, rt	**4k**	43%	Single Isomer
22l	3-Pent	L-Ala	PNP	**4**	$MgCl_2$, $(i\text{-Pr})_2NEt$, DMF, 50 °C	**4l**	42%	1.5 : 1
22m[5]	Neopent	L-Ala	PFP	**4**	*t*-BuMgCl, THF, DMF, rt	**4m**	10%	Single Isomer

22n	2-EtBu	D-Ala	PNP	**21**	$MgCl_2$, $(i\text{-Pr})_2NEt$, THF, 50 °C; conc. HCl, 0 °C	**4n**	66%	1.1 : 1
18b	Et	L-Ala	NA	**4**	$POCl_3$, $PO(OMe)_3$, Et_3N, rt	**4o**	16%	NA
18a	2-EtBu	L-Ala	NA	**4**	$POCl_3$, $PO(OMe)_3$, Et_3N, rt	**4p**	58%	NA

[1]Prodrug is an undetermined mixture of diastereoisomers unless otherwise indicated. [2]aa = amino acid, Ala = Alanine, Phe = Phenylalanine, AIB = 2-aminoisobutyrate, *c*-Bu = cyclobutyl, *c*-Pent = cyclopentyl, Pent = pentyl, Neopent = neopentyl, 2-EtBu = 2-ethylbutyl, PNP = *para*-nitrophenolate, PFP = pentafluorophenolate. [3]LG = Leaving Group. [4]Single *S*p isomer. [5]Reagent was a single unassigned isomer at phosphorus.

The monophosphate prodrugs can improve the potency of the parent nucleosides substantially by delivering the monophosphate into cells and effectively bypassing a rate limiting first phosphorylation step. The phenol and amino acid esters mask the negative charge of the mono-phosphate group enabling facile passive penetration into the cell. The prodrug breakdown is initiated by intracellular esterases (e.g. carboxy esterase 1, cathepsin A) that cleave the ester unraveling the carboxylate moiety, which then continues to breakdown to the monophosphate that serves as the prescursor to synthesis of the intracellular NTP.[17]

Prodrugs **4a-p** were evaluated toward EBOV in three cell lines and for human plasma stability (Table 3). In general the antiviral activity trends for EBOV across all three cell lines were similar supporting the efficient conversion of these prodrugs across multiple different cell types. A series of ethyl esters with differing amino acids (entries 2-5) established that the phenylalanine and alanine amino acids were the most promising (Table 1). Given the intended route of administration was intravenous, increasing lipophiliity beyond log D~2 was considered a potential issue due to solubility concerns. Therefore to improve potency the emphasis was placed on the less lipophilic and more commonly used alanine amino acid, with subsequent modification of the ester. Non-proximally branched esters of alanine with increasing log D ranging from 0.6 to 2.1 (entries 5, 11 and 12) demonstrated increased potency. Esters that contained proximal branching without cyclic motifs e.g. *i*-Pr, *t*-Bu, and 3-pentyl (entries 7,8 and 10 respectively) were generally less active, consistent with the increased steric hindrance that

likely slows down the cleavage rate by esterases. For example, the proximally branched 3-pentyl ester **4l** (entry 10) has comparable log D to that of the neopentyl analog **4m** (entry 11) yet much lower potency. In contrast, cyclic butyl and pentyl esters (entries 6 and 9 respectively) are more potent than **4l** despite the proximal branching and lower log D, although the potency in the HeLa cell assay was reduced. The D-Ala 2-EtBu mixture (entry 15) was less potent that the corresponding L-Ala analog mixture (entry 12) and the two bisphosphoramide prodrugs (entries 16 and 17) also had reduced activity compared to their monoamidate counterparts (entries 5 and 12 respectively). Thus, based on antiviral properties across HeLa and HMVEC cells, the most promising monophosphoramidate prodrugs were the neopentyl ester **4m** (single undefined isomer) and 2-EtBu ester mixture **4a**. The *S*p and *R*p isomers of **4a** (entries 14 and 15 respectively) were separated and found to be similar in potency, but both were marginally more potent than **4m**. For the intended iv route of administration, plasma stability was not deemed critical in the selection process provided sufficient stability ($t_{½}$ > 60 min) was maintained to allow loading of target cells harboring the virus during drug infusion. The selection of **4b** was made based on the high potency across multiple cell lines and the crystalline nature of the *S*p prodrug reagent **22b** that allowed rapid scale up for efficacy and IND enabling studies of the single *S*p isomer **4b**.

Table 3. Antiviral activity of prodrugs **4a-p**.[1]

Entry	Compound	Ester	aa[2]	EBOV EC_{50} HeLa (nM)	EBOV EC_{50} HMVEC[3] (nM)	EBOV EC_{50} Macro[4] (nM)	CC_{50} MT4 (μM)	Human Plasma $t_{1/2}$ (min)	LogD
1	**4**	-	-	>20000	780	>20000	>57	-	0.3
2	**4d**	Et	L-Phe	4380	587	270	15	1584	1.6

3	**4e**	Et	L-Val	7040	3151	-	>100	1584	1.2
4	**4f**	Et	AIB	8470	1585	-	>100	1584	0.9
5	**4g**	Et	L-Ala	2425	636	-	13	1584	0.6
6	**4h**	*c*-Bu	L-Ala	420	88	-	6	815	1.1
7	**4i**	*i*-Pr	L-Ala	1845	367	297	21	1561	1.1
8	**4j**	*t*-Bu	L-Ala	30410	3790	-	>100	1584	1.3
9	**4k**	*c*-Pent	L-Ala	633	160	120	8.8	1578	1.3
10	**4l**	3-Pent	L-Ala	1810	845	-	>100	860	1.6
11	**4m**	Neopent	L-Ala	168	92	-	3	700	1.7
12	**4a**	2-EtBu	L-Ala	170	121	100	2	195	2.1
13	**4c**	2-EtBu	L-Ala	80	53	111	3	234	2.0
14	**4b**	2-EtBu	L-Ala	100	53	86	1.7	69	2.1
15	**4n**	2-EtBu	D-Ala	550	518	729	42	1584	2.1
16	**4o**	Et	L-Ala	20420	9102	-	>53	-	<0.3
17	**4p**	2-EtBu	L-Ala	970	678	-	9	507	2.7

[1]Data is at least n ≥2 unless otherwise reported. [2]aa= Amino Acid, Ala = Alanine, Phe = Phenylalanine, AIB = 2-aminoisobutyrate, *c*-Bu = cyclobutyl, *c*-Pent = cyclopentyl, Pent = pentyl, 2-EtBu = 2-ethylbutyl. [3]HMVEC = TERT-immortalized human foreskin microvascular endothelial cells (ATCC-4025), [4]Macro = human macrophages.

In vivo efficacy evaluation of **4b** was conducted in monkeys since this represented the most relevant animal model of EVD with similar pathophysiology to the actual human disease. In addition, phosphoramidate esters are highly prone to plasma metabolism in rodents on account of high expression of plasma carboxylesterases[41] thereby excluding pilot efficacy studies in small animal models. Due to the high first pass hepatic extraction of phosphoramidates, oral administration was also not explored in favor of injectable routes of administration. Moreover, oral delivery in patients acutely infected with EBOV that are demonstrating symptoms of the disease may not be ideal because gasterointestinal symptoms may limit the dose that is effectively absorbed. Intravenous administration of **4b** in rhesus monkeys demonstrated rapid elimination of prodrug and appearance of parent nucleoside in systemic circulation (Figure 4a).

Figure 4. Concentration-time profiles following 10 mg/kg iv single dose slow bolus administration of **4b** in Rhesus (mean ± SD, n=3 per time point). (a) Plasma profile of prodrug **4b** (black circle) and parent nucleoside **4** (blue triangle). (b) Intracellular concentration of active metabolite **4tp** in PBMCs (green diamond) and estimated **4tp** EBOV IC_{50} = 5 μM (dashed black line).

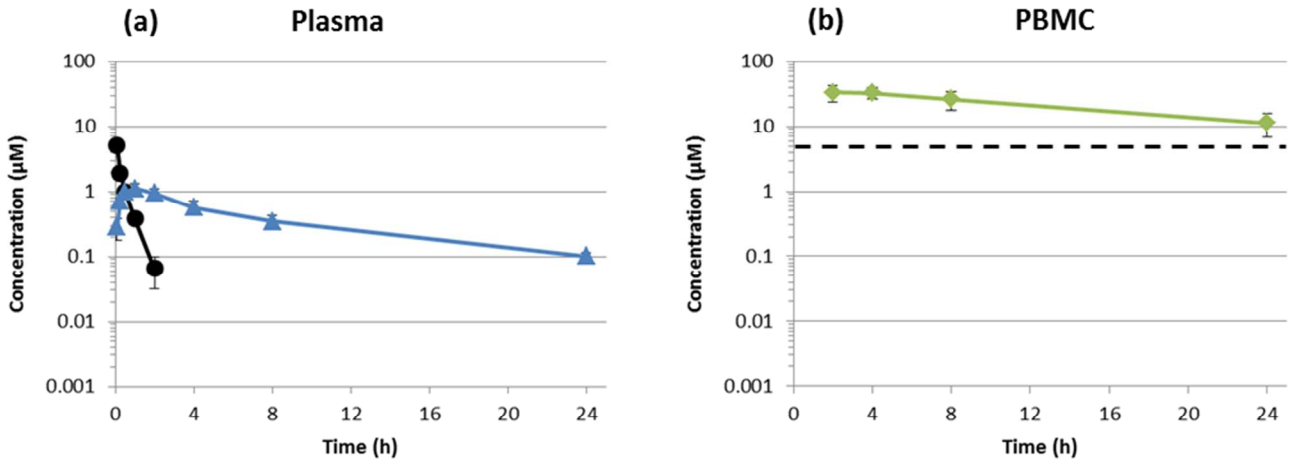

However **4b** also rapidly distributed to peripheral blood mononuclear cells (PBMCs) and triphosphate levels in PBMCs were elevated to a maximum within 2 h (Figure 4b). A dose of 10 mg/kg resulted in an estimated PBMC triphosphate level at 24 h that was several fold higher than the estimated IC_{50} of 5 μM for EBOV, with a half-life of 14 h similar to that measured in vitro in human macrophages. The long intracellular half-life of **4tp** supported once daily iv administration in the rhesus efficacy study and in the clinical program.

Preclinical in vivo efficacy for **4b** was conducted in a EBOV-infected rhesus challenge model. The overall strategy was to determine a maximally efficacious dose of **4b** that could be safely administered and to understand whether delayed time of treatment would be effective, a property that was considered critical for the successful clinical application of **4b**. These studies

have recently been published in full and will only be summarized here.[17] The starting dose of 3 mg/kg iv was modeled based on the NTP levels in rhesus PBMCs following 10 mg/kg iv dosing to have the potential for inhibiting Ebola viral replication in vivo. A correlation of the in vitro antiviral activity and intracellular metabolism described earlier suggested the 3mg/kg dose would produce NTP levels that exceed the estimated IC_{50} for most of the dosing interval. Compound **4b** was dosed iv at 3 mg/kg on day 0 or day 2 relative to EBOV inoculation, and continued once daily for 12 days. Systemic viremia was reduced and survival out to day 28 post infection was improved. Animals administered 3 mg/kg **4b** starting at day 0, had a survival rate of 33% whilst those initiated on day 3 had a 66% survival at 28 days. This encouraging data was then followed with a second study in which one arm explored dosing initiation on day 3 with 10 mg/kg daily for 12 days to assess whether increased dose compared to the 3 mg/kg result could be more efficacious. Two other arms explored an initial loading dose of 10 mg/kg on day 2 or day 3, followed by eleven 3 mg/kg daily maintenance doses. All the animals in the two arms in which **4b** treatments were initiated on day 3 (n=12 total) survived through day 28, the end of study. In the daily 10 mg/kg dosed group the effect on viremia was consistently greater than in any of the other groups and was below the limit of quantitation (8 x 10e4 RNA copies mL-1) in 4 of the 6 animals on days 5 and 7 relative to the vehicle-treated control in which the geometric mean exceeded 10e9 copies mL-1 at these time points. This data established the effectiveness of **4b** in treatment of EVD in NHPs and accelerated its progress into clinical development. In addition to the efficacy studies, distribution studies in cynomolgus monkeys using [^{14}C]**4b** at the same effective dose of 10 mg/kg established the presence of drug related products in the potential sanctuary sites for the virus including testes, epididymis, eyes and brain.[17] At 4 h post dose, the drug levels in the testes and epididymis exceeded those observed in plasma and even at 168 h

post dose detectable levels of drug related products were still observed in the testes. Exposure levels in the brain were lower than other tissues, including plasma at 4h, but were detectable above the plasma levels at 168 h indicating a long half-life of exposure in brain relative to plasma. These data supported the potential that **4b** treatment may also reduce persistence of virus in these sanctuary sites.

Safety and pharmacokinetics of **4b** administered as once-daily iv infusion were evaluated in single and multiple dose phase 1 clinical trials. No serious adverse effects of the drug were observed. During the course of the phase 1 studies two requests for a compassionate use of **4b** were received. The first case involved a healthcare worker who had survived acute infection but had relapsed with symptoms of acute meningoencephalytis.[42] Ebola virus was detected both systemically in plasma and in cerebrospinal fluid. When treated with monoclonal antibodies, the patient developed adverse reaction and was subsequently treated with supportive therapy and **4b** for a period of 14 days beginning with a dose of 150 mg and then increasing to 225 mg after 2 daily infusions. No serious adverse effects related to drug were observed. The patient recovered and cleared the virus from both plasma and CNS although without proper control or natural history data to compare, it is not clear whether the antiviral therapy was effective. The second case involved a newborn infant congenitally infected with EBOV and treated with monoclonal antibodies, blood transfusion and subsequently **4b**.[43] The infant recovered and was eventually declared free of Ebola virus after repeated testing failed to detect viremia. The unprecedented scale of the West African epidemic and the ability to reduce mortality rates through supportive therapy has resulted in many survivors of EVD. The persistence of virus sequelae in survivors in multiple body compartments has now been documented in addition to secondary sexual transmission via virus in genital secretions.[4] This has prompted the initiation of randomized,

blinded, placebo-controlled phase 2 study (PREVAIL IV) which plans to enroll at least 60 adult male survivors to receive either 100 mg **4b** or placebo once-daily over 5 days to assess the effect of **4b** therapy on the viral shedding in semen.[44] The results of this study could provide the first evidence as to the potential of **4b** to reduce virus replication in humans.

CONCLUSION

The recent EBOV outbreak prompted the urgent need for antiviral therapeutics for the treatment of EVD. We identified a promising nucleotide therapeutic **4b** through initial screening and subsequent optimization of the prodrug moiety for iv administration. The partnership with government organizations, including CDC and USAMRIID, that generated the screening data and conducted the rhesus efficacy studies was critical to the successful identification of **4b**. Also of importance was the significant chemistry effort that rapidly identified a more efficient route to the parent compound **4** and the ability to prepare, through crystallization of a key reagent, the single *S*p phosphorus diastereoisomer **4b** for in vivo model studies. The active triphosphate delivered by the prodrug has low micromolar polymerase activity toward EBOV, high selectivity for the viral polymerase compared to host polymerases, and a long intracellular half-life supporting once daily administration. Parenteral treatment with **4b** in EBOV infected NHPs at 10 mg/kg over 12 days demonstrated a substantial antiviral effect along with 100% survival. Based on its promising potential, and preliminary safety data from phase 1 studies, regulatory authorities approved the compassionate use of **4b** in two cases including an newborn infant with EVD. Further clinical data on **4b** is being collected in the phase 2 PREVAIL IV study that aims to assess the ability of **4b** to reduce persistence of EBOV in sanctuary sites of survivors.

EXPERIMENTAL

All organic compounds were synthesized at Gilead Sciences, Inc (Foster City, CA) unless otherwise noted. Commercially available solvents and reagents were used as received without further purification. Nuclear magnetic resonance (NMR) spectra were recorded on a Varian Mercury Plus 400 MHz at room temperature, with tetramethylsilane as an internal standard. Proton nuclear magnetic resonance spectra are reported in parts per million (ppm) on the δ scale and are referenced from the residual protium in the NMR solvent (chloroform-d_1: δ 7.26, methanol-d_4: δ 3.31, DMSO-d_6: δ 2.50). Data is reported as follows: chemical shift [multiplicity (s = singlet, d = doublet, t = triplet, q = quartet, p = pentet, sep = septet, m = multiplet, br = broad, app = apparent), coupling constants (*J*) in Hertz, integration. Carbon-13 nuclear magnetic resonance spectra are reported in parts per million on the δ scale and are referenced from the carbon resonances of the solvent (chloroform-d_1: δ 77.16, methanol-d_4: δ 49.15, DMSO-d_6: δ 39.52). Data is reported as follows: chemical shift. No special nomenclature is used for equivalent carbons. Phosphorus-31 nuclear magnetic resonance spectra are reported in parts per million on the δ scale. Data is reported as follows: chemical shift [multiplicity (s = singlet, d = doublet, t = triplet), coupling constants (*J*) in Hertz. No special nomenclature is used for equivalent phosphorus resonances. Analytical thin–layer chromatography was performed using Merck KGaA Silica gel 60 F_{254} glassplates with UV visualization. Preparative normal phase silica gel chromatography was carried out using a Teledyne ISCO CombiFlash Companion instrument with silica gel cartridges. Purities of the final compounds were determined by high-performance liquid chromatography (HPLC) and were greater than 95% unless otherwise noted. HPLC conditions to assess purity were as follows: Agilent 1100 Series HPLC, Phenominex Kinetex C18, 2.6 µm 100Å, 100 × 4.6 mm column; 2-98% gradient of 0.1% trifluoroacetic acid

in water and 0.1% trifluoroacetic acid in acetonitrile; flow rate, 1.5 mL/min; acquisition time, 8.5 min; wavelength, UV 214 and 254 nm. High-resolution mass spectrometry (HRMS) was performed on an Agilent model 6230 Accurate Mass Time of Flight Mass Spectrometer featuring Agilent Jet Stream Thermal Focusing Technology, with an Agilent 1200 Rapid Resolution HPLC. HRMS chromatography was performed using an Agilent Zorbax Eclipse Plus C18 RRHD 1.8 μm, 2.1 × 50 mm column at 30 °C, with a 10-90% gradient of 0.05% trifluoroacetic acid in water and 0.05% trifluoroacetic acid in acetonitrile. LC-MS was conducted on a Thermo Finnigan MSQ Std using electrospray positive and negative $[M + 1]^+$ and $[M - 1]^-$, and a Dionex Summit HPLC System (model: P680A HPG) equipped with a Gemini 5 u C18 110A column (30 mm × 4.60 mm), eluting with 0.05% formic acid in 1% acetonitrile/waterand 0.05% formic acid in 99% acetonitrile/water. Optical rotations were recorded on a Jasco P-2000 Polarimeter.

The synthesis, characterization data, and associated references for the following compounds are provided in supporting information: **4, 4a, 7-11, 9a, 11a, 12-13, 13a, 13b, 4tp, 13tp, 16-17, 18a, 19, 21,** and **22a-n.**

(*S*)-2-ethylbutyl 2-(((*S*)-(((2*R*,3*S*,4*R*,5*R*)-5-(4-aminopyrrolo[2,1-*f*][1,2,4]triazin-7-yl)-5-cyano-3,4-dihydroxytetrahydrofuran-2-yl)methoxy)(phenoxy)phosphoryl)amino)propanoate (4b). Compound **4b** was prepared from **4** and **22b** as described previously.[17] ^{1}H NMR (400 MHz, methanol-d_4): δ 7.86 (s, 1H), 7.33 – 7.26 (m, 2H), 7.21 – 7.12 (m, 3H), 6.91 (d, J = 4.6 Hz, 1H), 6.87 (d, J = 4.6 Hz, 1H), 4.79 (d, J = 5.4 Hz, 1H), 4.43 – 4.34 (m, 2H), 4.28 (ddd, J = 10.3, 5.9, 4.2 Hz, 1H), 4.17 (t, J = 5.6 Hz, 1H), 4.02 (dd, J = 10.9, 5.8 Hz, 1H), 3.96 – 3.85 (m, 2H), 1.49 – 1.41 (m, 1H), 1.35 – 1.27 (m, 8H), 0.85 (t, J = 7.4 Hz, 6H). ^{13}C-NMR (100 MHz, methanol-d_4): δ 174.98, 174.92, 157.18, 152.14, 152.07, 148.27, 130.68, 126.04, 125.51, 121.33, 121.28, 117.90, 117.58, 112.29, 102.60, 84.31,

84.22, 81.26, 75.63, 71.63, 68.10, 67.17, 67.12, 51.46, 41.65, 24.19, 20.56, 20.50, 11.33, 11.28.; ^{31}P-NMR (162 MHz, methanol-d_4): δ 3.66 (s); HRMS (*m*/*z*): $[M]^+$ calcd for $C_{27}H_{35}N_6O_8P$, 602.2254; found, 602.2274. $[\alpha]^{21}_D$ –21 (*c* 1.0, MeOH).

(*S*)-2-ethylbutyl 2-(((*R*)-(((2*R*,3*S*,4*R*,5*R*)-5-(4-aminopyrrolo[2,1-*f*][1,2,4]triazin-7-yl)-5-cyano-3,4-dihydroxytetrahydrofuran-2-yl)methoxy)(phenoxy)phosphoryl)amino)propanoate (4c). Compound **4c** was prepared from **4a** by chiral chromatography. **4a** was dissolved in acetonitrile. The resulting solution was loaded onto Lux Cellulose-2 chiral column, equilibrated in acetonitrile, and eluted with isocratic acetonitrile/methanol (95:5 vol/vol). The first eluting compound was the *R*p diastereomer **4c**, and the second eluting compound was the *S*p diastereomer **4b.** ^{1}H NMR (400 MHz, methanol-d_4) δ 8.05 (s, 1H), 7.36 (d, *J* = 4.8 Hz, 1H), 7.29 (br t, *J* = 7.8 Hz, 2H), 7.19 – 7.13 (m, 3H), 7.11 (d, *J* = 4.8 Hz, 1H), 4.73 (d, *J* = 5.2 Hz, 1H), 4.48 – 4.38 (m, 2H), 4.37 – 4.28 (m, 1H), 4.17 (t, *J* = 5.6 Hz, 1H), 4.08 – 3.94 (m, 2H), 3.94 – 3.80 (m, 1H), 1.48 (sep, *J* = 12.0, 6.1 Hz, 1H), 1.34 (p, *J* = 7.3 Hz, 4H), 1.29 (d, *J* = 7.2 Hz, 3H), 0.87 (t, *J* = 7.4 Hz, 6H). ^{31}P NMR (162 MHz, methanol-d_4) δ 3.71 (s). MS *m/z* 603.1 [M+1]. $[\alpha]^{21}_D$ –46 (*c* 1.0, MeOH).

(2*S*)-ethyl-2-(((((2*R*,3*S*,4*R*,5*R*)-5-(4-aminopyrrolo[2,1-*f*][1,2,4]triazin-7-yl)-5-cyano-3,4-dihydroxytetrahydrofuran-2-yl)methoxy)(phenoxy)phosphoryl)amino)-3-phenylpropanoate (4d). Compound **4** (0.030 g, 0.103 mmol) was dissolved in DMF (1 mL) and then THF (0.5 mL) was added. *t*-BuMgCl (1M/THF, 154.5 µL, 0.154 µmol) was added to the reaction in a drop-wise manner with vigorous stirring. The resulting white slurry was stirred at rt for about 30 min. A solution of compound **22d** (0.058 g, 0.124 mmol) in THF (1 mL) was added

in a drop-wise manner to the reaction at rt. The reaction progress was monitored by LC-MS. When the reaction progressed to 50% conversion, the reaction was cooled in an ice bath and quenched with glacial acetic acid (70 μL). The reaction was concentrated and the crude residue was purified by reverse phase preparatory HPLC to afford compound **4d** (22 mg, 34%, as a 2.6:1 mixture of diastereomers at phosphorus). ^{1}H NMR (400 MHz, DMSO-d_6) δ 7.91 (d, J = 4 Hz, 1H), 7.90 (br s, 2H), 7.09-7.30 (m, 8H), 7.01, (t, J = 8.2 Hz, 2H), 6.89 (d, J = 4.4 Hz, 1H), 6.82 (t, J = 4.4 Hz, 1H), 6.27 (m, 1H), 6.14 (m, 1H), 5.34 (m, 1H), 4.62 (t, J = 5.6 Hz, 1H), 4.15 (m, 1H), 3.78-4.01 (m, 6H), 2.92 (m, 1H), 2.78 (m, 1H), 1.04 (m, 3H). ^{31}P NMR (162 MHz, DMSO-d_6) δ 3.69 (s), 3.34 (s). MS m/z = 623.0 [M+1].

(2*S*)-ethyl-2-(((((2*R*,3*S*,4*R*,5*R*)-5-(4-aminopyrrolo[2,1-*f*][1,2,4]triazin-7-yl)-5-cyano-3,4-dihydroxytetrahydrofuran-2-yl)methoxy)(phenoxy)phosphoryl)amino)-3-methylbutanoate (4e). Compound **4** (0.040 g, 0.14 mmol) was dissolved in NMP (1.5 mL) and then THF (0.25 mL) was added. This solution was cooled in an ice bath and *t*-BuMgCl (1M/THF, 425.7 μL, 0.426 μmol) was added in a drop-wise manner with vigorous stirring. The ice bath was removed and the resulting white slurry was stirred at rt for about 15 min. A solution of compound **22e** (0.081 g, 0.192 mmol) in THF (0.5 mL) was added in a drop-wise manner to the reaction at rt. The reaction progress was monitored by LC-MS. When the reaction progressed to 50% conversion, the reaction was cooled in an ice bath and quenched with glacial acetic acid (70 μL). The reaction was concentrated and crude residue was semi-purified from the residue by reverse phase HPLC. The semi-pure material was further purified by silica gel column chromatography (eluent: 100% EtOAc ramping to 10% MeOH in EtOAc) to afford compound **4e** (0.034 g, 43% as a 1.8:1 mixture of diastereomers). ^{1}H NMR (400 MHz, DMSO-d_6) δ 7.91 (d, J = 1.6 Hz, 1H), 7.88 (br s, 2H), 7.32 (m, 2H), 7.15 (m, 3H), 6.90 (t, J = 4.2 Hz, 1H), 6.84 (d, J = 4.8 Hz, 1H),

6.26 (dd, *J* = 13.4, 6.2 Hz, 1H), 5.87 (q, *J* = 11.2 Hz, 1H), 5.35 (m, 1H), 4.64 (m, 1H), 4.25 (m, 2H), 3.93-4.15 (m, 4H), 3.45 (m, 1H), 1.87 (m, 1H), 1.09-1.16 (m, 3H), 0.70-0.83 (m ,6H). ^{31}P NMR (162 MHz, DMSO-d_6) δ 4.59 (s), 4.47 (s). MS *m/z* = 575.02 [M+1].

Ethyl 2-(((((2*R*,3*S*,4*R*,5*R*)-5-(4-aminopyrrolo[2,1-*f*][1,2,4]triazin-7-yl)-5-cyano-3,4-dihydroxytetrahydrofuran-2-yl)methoxy)(phenoxy)phosphoryl)amino)-2-methylpropanoate (4f). Compound **4** (66 mg, 0.23 mmol) was dissolved in NMP (2.0 mL) and the mixture was cooled to about 0 °C. *t*-BuMgCl (1.0M in THF, 0.34 mL, 0.34 mmol) was then added and the resulting mixture was stirred at 0 °C for about 30 min. A solution of compound **22f** (139 mg, 0.34 mmol) in THF (1.0 mL) was then added, and the reaction mixture was heated to about 50 °C. After about 2 h, the reaction was cooled to rt and quenched with acetic acid and methanol. The resulting mixture was concentrated under reduced pressure and purified by preparatory reverse phase HPLC to afford compound **4f** (32 mg, 25% as a 1.5:1 mixture of diastereomers). ^{1}H NMR (400 MHz, DMSO-d_6) δ 7.89 (m, 3H), 7.31 (q, *J* = 8.1 Hz, 2H), 7.22 – 7.05 (m, 3H), 6.87 (d, *J* = 4.5, 1H), 6.80 (d, *J* = 4.5 Hz, 1H), 6.27 (d, *J* = 11.7, 1H), 5.81 (d, *J* = 9.7, 1H), 5.35 (d, *J* = 5.6 Hz, 1H), 4.64 (dt, *J* = 9.0, 5.6 Hz, 1H), 4.24 (m, 2H), 4.11 (m, 1H), 4.04 – 3.90 (m, 3H), 1.39 – 1.23 (m, 6H), 1.10 (t, *J* = 7.1, 3H). ^{31}P NMR (162 MHz, DMSO-d_6) δ 2.45, 2.41. MS *m/z* = 561.03 [M+1].

Ethyl ((((2*R*,3*S*,4*R*,5*R*)-5-(4-aminopyrrolo[2,1-*f*][1,2,4]triazin-7-yl)-5-cyano-3,4-dihydroxytetrahydrofuran-2-yl)methoxy)(phenoxy)phosphoryl)-L-alaninate (4g). Compound **4** (50 mg, 0.17 mmol) was dissolved in NMP-THF (1:1 mL)) and cooled with ice bath. *t*-BuMgCl (1.0M in THF, 0.257 mL, 0.257 mmol) was then added over about 5 min. The

resulting mixture was allowed to warm to rt and was stirred for about 30 min. Then a solution of compound **22g** (74.6 mg, 0.189 mmol) in THF (2 mL) was added. After about 30 min, the reaction mixture was purified by preparatory reverse phase HPLC. Fractions containing the desired product were further purified with silica gel chromatography (eluent: 0-20% methanol in dichloromethane) to afford compound **4g** (23 mg, 24% as a 2.5:1 mixture of diastereomers). ^{1}H NMR (400 MHz, methanol-d_4) δ 7.76 (d, J = 6.0 Hz, 1H), 7.25 – 7.14 (m, 2H), 7.11 – 6.99 (m, 3H), 6.87 – 6.72 (m, 2H), 4.70 (d, J = 5.4 Hz, 1H), 4.39 – 4.24 (m, 2H), 4.20 (dddd, J = 9.7, 7.9, 5.1, 2.8 Hz, 1H), 4.10 (dt, J = 12.8, 5.5 Hz, 1H), 4.06 – 3.91 (m, 2H), 3.72 (ddq, J = 14.3, 9.3, 7.1 Hz, 1H), 1.17 (dd, J = 7.1, 1.0 Hz, 1H), 1.14 – 1.06 (m, 5H). ^{31}P NMR (162 MHz, methanol-d_4) δ 3.73, 3.68. MS m/z = 547 [M+1].

(2*S*)-cyclobutyl 2-(((((2*R*,3*S*,4*R*,5*R*)-5-(4-aminopyrrolo[2,1-*f*][1,2,4]triazin-7-yl)-5-cyano-3,4-dihydroxytetrahydrofuran-2-yl)methoxy)(phenoxy)phosphoryl)amino)propanoate (4h). Compound **4** (58 mg, 0.20 mmol) was mixed with compound **22h** (101 mg, 0.240 mmol) in 2 mL of anhydrous DMF. Magnesium chloride (42 mg, 0.44 mmol) was added in one portion. The reaction mixture was heated to about 50 °C. *N,N*-Diisopropylethylamine (87 µL, 0.5 mmol) was added, and the reaction was stirred for about 2 h at about 50 °C. The reaction mixture was cooled to room temperature, was diluted with ethyl acetate and was washed with 5% aqueous citric acid solution followed by saturated aqueous sodium chloride solution. The organic layer was then dried over anhydrous sodium sulfate and concentrated under reduced pressure. The crude residue was purified with silica gel column (eluent: 0-5% methanol in dichloromethane) to afford compound **4h** (42 mg, 37% yield, as a 3:2 mixture of diastereomers). ^{1}H NMR (400 MHz, methanol-d_4) δ 7.85 (m, 1H), 7.34 – 7.22 (m, 2H), 7.22 – 7.08 (m, 3H), 6.94 – 6.84 (m,

2H), 4.95 – 4.85 (m, 1H), 4.79 (m, 1H), 4.46 – 4.34 (m, 2H), 4.34 – 4.24 (m, 1H), 4.19 (m, 1H), 3.81 (m, 1H), 2.27 (m, 2H), 2.01 (m, 2H), 1.84 – 1.68 (m, 1H), 1.62 (m, 1H), 1.30 – 1.16 (m, 3H). ^{31}P NMR (162 MHz, methanol-d_4) δ 3.70, 3.65. MS *m/z* = 573.0 [M+1].

(*S*)-Isopropyl 2-(((*R*)-(((2*R*,3*S*,4*R*,5*R*)-5-(4-aminopyrrolo[2,1-*f*][1,2,4]triazin-7-yl)-5-cyano-3,4-dihydroxytetrahydrofuran-2-yl)methoxy)(phenoxy)phosphoryl)amino)propanoate (4i). Compound **4** (60.0 mg, 206 μmol) was dissolved in NMP (0.28 mL). THF (0.2 mL) was added followed by *tert*-butyl magnesium chloride (1.0M solution in tetrahydrofuran, 0.309 mL) at rt under an argon atmosphere. After 20 min, a solution of compound **22i** (81 mg, 206 μmol) in THF (0.2 mL) was added, and the resulting mixture was warmed to about 50 °C. After 3 h, the reaction mixture was allowed to cool to rt and was purified directly by preparatory HPLC to afford compound **4i** (44 mg, 38% as a single diastereomer). ^{1}H NMR (400 MHz, methanol-d_4) δ 7.86 (s, 1H), 7.34 – 7.26 (m, 2H), 7.21 – 7.12 (m, 3H), 6.91 (d, *J* = 4.6 Hz, 1H), 6.87 (d, *J* = 4.6 Hz, 1H), 4.92 (septet, *J* = 6.3 Hz, 1H), 4.80 (d, *J* = 5.4 Hz, 1H), 4.43 – 4.34 (m, 1H), 4.33 – 4.24 (m, 1H), 4.18 (t, *J* = 5.6 Hz, 1H), 3.82 (dq, *J* = 9.7, 7.1 Hz, 2H), 1.27 (dd, *J* = 7.1, 1.0 Hz, 3H), 1.18 (dd, *J* = 6.3, 4.8 Hz, 6H). ^{31}P NMR (162 MHz, methanol-d_4) δ 3.72 (s). MS *m/z* = 561.11 [M+1].

***tert*-Butyl ((((2*R*,3*S*,4*R*,5*R*)-5-(4-aminopyrrolo[2,1-*f*][1,2,4]triazin-7-yl)-5-cyano-3,4-dihydroxytetrahydrofuran-2-yl)methoxy)(phenoxy)phosphoryl)-L-alaninate (4j).** To a mixture of intermediate **4** (80 mg, 0.28 mmol), intermediate **22j** (174 mg, 0.41 mmol), and $MgCl_2$ (39 mg, 0.41 mmol) in DMF (4 mL) was added *N,N*-diisopropylethylamine (0.12 mL, 0.69 mmol) dropwise at room temperature. The reaction mixture was stirred at 50 °C for 1 h and

was cooled to rt. The resulting mixture was concentrated under reduced pressure to approximately 2 mL volume and was purified by reverse phase preparative HPLC. Fractions containing the desired product were combined and further purified by silica gel column chromatography (eluent: 0-20% methanol in methylene chloride) to afford compound **4j** (51 mg, 32%, 1.5:1 diastereomeric mixture). ^{1}H NMR (400 MHz, methanol-d_4) δ 7.86 (s, 0.4H), 7.84 (s, 0.6H), 7.28 (m, 2H), 7.21 – 7.10 (m, 3H), 6.96 – 6.83 (m, 2H), 4.79 (m, 1H), 4.46 – 4.34 (m, 2H), 4.28 (m, 1H), 4.22 – 4.13 (m, 1H), 3.81 – 3.64 (m, 1H), 1.40 (m, 9H), 1.22 (m, 3H). ^{31}P NMR (162 MHz, methanol-d_4) δ 3.79 (s). MS *m/z* = 575 [M+1].

(2*S*)-cyclopentyl 2-(((((2*R*,3*S*,4*R*,5*R*)-5-(4-aminopyrrolo[2,1-*f*][1,2,4]triazin-7-yl)-5-cyano-3,4-dihydroxytetrahydrofuran-2-yl)methoxy)(phenoxy)phosphoryl)amino) propanoate (4k). Compound **4** (100 mg, 0.34 mmol) was dissolved in THF (2 mL) and cooled under ice water bath. Then 1M *t*-BuMgCl (0.52 mL, 0.77 mmol) was added dropwise slowly. The resulting mixture was stirred for about 30 min at rt. Then compound **22k** (247 mg, 0.52 mmol) in THF (2 mL) was added over about 5 min and the resulting mixture was stirred for about 24 h at rt. The resulting mixture was diluted with ethyl acetate, cooled under ice-water bath, treated with aq $NaHCO_3$ (2 mL), washed with brine, dried with sodium sulfate, and concentrated under reduced pressure. The resulting mixture was purified by silica gel column chromatography (eluent: 0-20% methanol in dichloromethane) followed by reverse phase preparatory HPLC to afford compound **4k** (47 mg, 23% as a 27:1 mixture of diastereomers). ^{1}H NMR (400 MHz, methanol-d_4) δ 7.85 (s, 1H), 7.33 – 7.22 (m, 2H), 7.14 (tdd, *J* = 7.6, 2.1, 1.1 Hz, 3H), 6.95 – 6.87 (m, 2H), 5.13 – 5.00 (m, 1H), 4.78 (d, *J* = 5.4 Hz, 1H), 4.48 – 4.35 (m, 2H), 4.30 (ddd, *J* = 10.6,

5.7, 3.6 Hz, 1H), 4.19 (t, *J* = 5.4 Hz, 1H), 3.78 (dq, *J* = 9.2, 7.1 Hz, 1H), 1.81 (dtd, *J* = 12.5, 5.9, 2.4 Hz, 2H), 1.74 – 1.49 (m, 6H), 1.21 (dd, *J* = 7.1, 1.2 Hz, 3H). MS *m/z* = 587 [M+1].

Pentan-3-yl ((((2*R*,3*S*,4*R*,5*R*)-5-(4-aminopyrrolo[2,1-*f*][1,2,4]triazin-7-yl)-5-cyano-3,4-dihydroxytetrahydrofuran-2-yl)methoxy)(phenoxy)phosphoryl)-L-alaninate (4l). To a mixture of compound **4** (80 mg, 0.28 mmol), **22l** (170 mg, 0.39 mmol), and $MgCl_2$ (39 mg, 0.41 mmol) in DMF (4 mL) was added *N,N*-diisopropylethylamine (0.12 mL, 0.69 mmol) dropwise at rt. The resulting mixture was stirred at 50 °C for 1 h, concentrated to approximately 2 mL volume and purified by reverse phase preparative HPLC to afford compound **4l** (68 mg, 42%, 1.5:1 diastereomeric mixture). ^{1}H NMR (400 MHz, methanol-d_4) δ 7.86 (s, 0.4 H), 7.85 (s, 0.6 H), 7.33 – 7.23 (m, 2H), 7.21 – 7.08 (m, 3H), 6.95 – 6.84 (m, 2H), 4.79 (m, 1H), 4.69 (m, 1H), 4.47 – 4.34 (m, 2H), 4.34 – 4.24 (m, 1H), 4.19 (m, 1H), 3.85 (m, 1H), 1.64 – 1.42 (m, 4H), 1.29 (dd, *J* = 7.0, 1.1 Hz, 1.1 H), 1.23 (dd, *J* = 7.2, 1.3 Hz, 1.9H), 0.91 – 0.76 (m, 6H). ^{31}P NMR (162 MHz, methanol-d_4) δ 3.71, 3.69. MS *m/z* = 589 [M+1].

(*S*)-Neopentyl 2-(((S)-(((2R,3S,4R,5R)-5-(4-aminopyrrolo[2,1-f][1,2,4]triazin-7-yl)-5-cyano-3,4-dihydroxytetrahydrofuran-2-yl)methoxy)(phenoxy)phosphoryl)amino)propanoate (4m) Compound **4** (100 mg, 0.34 mmol) was dissolved in THF (2 mL) and cooled under ice water bath. Then 1M t-BuMgCl (0.52 mL, 0.77 mmol) was added dropwise slowly. The resulting mixture was stirred for 30 min at room temperature. Then compound **22m** (248 mg, 0.52 mmol) was added over 5 min and the resulting mixture was stirred for 24h at room temperature, diluted with EtOAc, cooled under ice-water bath, treated with aq $NaHCO_3$ (2mL), washed with brine, dried with sodium sulfate, and concentrated *in vacuo*. The resulting mixture was purified by

silica gel column chromatography (MeOH 0 to 20% in DCM) and prep-HPLC (acetonitrile 10 to 80% in water) to give Compound **4m** (12 mg, 10% as a single diastereomer).

1H NMR (400 MHz, CD_3OD) δ 7.86 (s, 1H), 7.36 – 7.24 (m, 2H), 7.23 – 7.10 (m, 3H), 6.96 – 6.85 (m, 2H), 4.78 (d, *J* = 5.4 Hz, 1H), 4.38 (tdd, *J* = 10.0, 4.9, 2.5 Hz, 2H), 4.32 – 4.24 (m, 1H), 4.17 (t, *J* = 5.6 Hz, 1H), 3.91 (dq, *J* = 9.8, 7.1 Hz, 1H), 3.81 (d, *J* = 10.5 Hz, 1H), 3.69 (d, *J* = 10.5 Hz, 1H), 1.31 (dd, *J* = 7.2, 1.1 Hz, 3H), 0.89 (s, 9H).

MS m/z = 589 $(M+1)^+$

2-Ethylbutyl ((((2*R*,3*S*,4*R*,5*R*)-5-(4-aminopyrrolo[2,1-*f*][1,2,4]triazin-7-yl)-5-cyano-3,4-dihydroxytetrahydrofuran-2-yl)methoxy)(phenoxy)phosphoryl)-D-alaninate (4n).

Compound **21** (50 mg, 0.15 mmol) was dissolved in anhydrous tetrahydrofuran (5 mL) and stirred under atmospheric argon. Compound **22n** (75 mg, 0.17 mmol) was added followed by magnesium chloride (21 mg, 0.23 mmol), and the reaction was warmed to 50 °C and stirred for 30 min. *N,N*-diisopropylethylamine (65.0 µL, 0.375 mmol) was added dropwise, and the reaction mixture was stirred for 3 h at 50 °C. The reaction mixture was then cooled in an ice bath and 12N HCl(aq) (175 µL) was added dropwise. The ice bath was removed and the reaction mixture was stirred at rt for 4 h. The reaction mixture was diluted with ethyl acetate (15 mL) and cooled in an ice bath. 1N NaOH(aq) was added slowly to give pH of 10. The organic layer was then washed with 5% aqueous sodium carbonate solution and then saturated aqueous sodium chloride solution. The organic layer was then dried over anhydrous sodium sulfate and concentrated under reduced pressure. The crude residue was purified with silica gel column chromatography (eluent: 0-10% methanol in dichloromethane) to afford compound **4n** (60 mg, 66% yield as a 1.1:1 diastereomeric mixture). ^{1}H NMR (400 MHz, methanol-d_4) δ 7.87 – 7.83

(m, 1H), 7.37 – 7.22 (m, 2H), 7.22 – 7.04 (m, 3H), 6.96 – 6.79 (m, 2H), 4.82 – 4.75 (m, 1H), 4.45 – 4.23 (m, 3H), 4.18 (m, 1H), 4.06 – 3.85 (m, 3H), 1.52 – 1.38 (m, 1H), 1.38 – 1.24 (m, 7H), 0.85 (m, 6H). ^{31}P NMR (162 MHz, methanol-d_4) δ 3.87, 3.55. MS *m/z* = 603.1 [M+1].

(2*S*,2'*S*)-diethyl 2,2'-((((2*R*,3*S*,4*R*,5*R*)-5-(4-aminopyrrolo[1,2-*f*][1,2,4]triazin-7-yl)-5-cyano-3,4-dihydroxytetrahydrofuran-2-yl)methoxy)phosphoryl)bis(azanediyl) dipropanoate (4o). Compound **4** (14.6 mg, 0.05 mmol) was dissolved in anhydrous trimethyl phosphate (0.5 mL) and stirred under N_2(g) at rt. $POCl_3$ (9.2 µL, 0.1 mmol) was added and the mixture stirred for about 60 min. Alanine ethyl ester hydrochloride **18b** (61 mg, 0.4 mmol, Aldrich CAS#1115-59-9) and then Et_3N (70 µL, 0.5 mmol) was added. The resultant mixture was stirred for about 15 min. and then additional Et_3N (70 µl, 0.5 mmol) was added to give a solution pH of 9-10. The mixture was stirred for about 2 h. and then diluted with ethyl acetate, washed with saturated aqueous $NaHCO_3$ solution followed by saturated aqueous NaCl solution. The organic layer was dried over anhydrous sodium sulfate and concentrated under reduced pressure. The residue was purified by reverse phase preparative HPLC to afford compound **4o** (5.5 mg, 16%). ^{1}H NMR (400 MHz, methanol-d_4) δ 8.13 (s, 1H), 7.41 (d, *J* = 4.8 Hz, 1H), 7.18 (d, *J* = 4.8 Hz, 1H), 4.78 (d, *J* = 5.6 Hz, 1H), 4.36 (m, 1H), 4.25-4.08 (m, 7H), 3.83 (m, 2H), 1.33-1.23 (m, 12H). ^{31}P NMR (121.4 MHz, methanol-d_4) δ 13.8. MS *m/z* 570.0 [M+1].

(2*S*,2'*S*)-di(2-ethylbutyl) 2,2'-((((2*R*,3*S*,4*R*,5*R*)-5-(4-aminopyrrolo[1,2-*f*][1,2,4]triazin-7-yl)-5-cyano-3,4-dihydroxytetrahydrofuran-2-yl)methoxy)phosphoryl)bis(azanediyl) dipropanoate (4p). To a suspension of compound **4** (52 mg, 0.18 mmol) and solid sodium bicarbonate (53 mg) in trimethyl phosphate (1.5 mL) at 0 °C was added $POCl_3$ (120 mg, 0.783

mmol). The mixture was stirred at 0 °C for 3 h, at which point a solution of **18a** (790 mg, 4.56 mmol) in MeCN (1 mL) was then added. The reaction mixture was stirred at 0 °C for 0.5 h, then triethylamine (0.1 mL) was added and stirred at rt for 0.5 h. The reaction mixture was diluted with ethyl acetate (10 mL), washed with water (10 mL), and was concentrated under reduced pressure. The residue was purified by silica gel column chromatography (eluent: 50-100% ethyl acetate in hexanes gradient followed by 0-10% methanol in ethyl acetate gradient) to afford compound **4p** (71 mg, 58%). ^{1}H NMR (400 MHz, methanol-d_4): δ 7.88 (s, 1H), 6.95 (d, J = 4.8 Hz, 1H), 6.89 (d, J = 4.4 Hz, 1H), 4.85 (d, J = 5.6 Hz, 1H), 4.32-4.35 (m, 1H), 4.12-4.26 (m, 3H), 4.04-4.09 (m, 2H), 3.94-3.98 (m, 2H), 3.79-3.89 (m, 2H), 1.44-1.54 (m, 2H), 1.27-1.39 (m, 14H), 0.89 (t, J = 7.2 Hz, 12H). ^{31}P NMR (400 MHz, methanol-d_4): δ 13.83. MS m/z = 682.1 [M+1].

Supporting Information: Assay Methods, Molecular Modeling with RSV, Marburg and Sudan viruses, compound synthesis, single crystal X-Ray structure information and molecular formula strings (CSV) are available in Supporting Information.

Accession Codes: The Cambridge Crystallographic Data Center (CCDC) numbers for the X-Ray structures of compound **22b** and **4b** are 1445315 and 1525480 respectively.

Homology models: HIV (1RTD[32b]) and HCV (4WTG[32c]) X-Ray structures were used to generate the EBOV model for **4tp** and **13tp**. Please see the Supporting Information for the Molecular Modeling information.

Corresponding Author Information: richard.mackman@gilead.com. Tel: 650 522 5258.

Acknowledgement: We acknowledge the contributions of the following individuals at USAMRIID for participation in vivo studies, J. Wells, K. Stuthman, N. Lackemeyer, S. Van Tongeren, G. Donnelly, J. Steffens, A. Shurtleff, L. Gomba, J. Benko; scientific input, L. Welch, T. Bocan, A. Duplantier, R. Panchal, C. Kane, D. Mayers (currently of Cocrystal Pharma, Inc.); and for services performed, S Tritsch, C. Retterer, D. Gharaibeh, T. Kenny, B. Eaton, G. Gomba, J. Nuss and C. Rice. From Gilead Sciences we acknowledge K. Wang, K. Brendza, T. Alfredson and L. Serafini who assisted with analytical methods, S. Bondy and R. Seemayer procured key raw materials, L. Heumann, R. Polniaszeck, E. Rueden, A. ChtChemelinine, K. Brak and B. Hoang contributed to synthesis, Yelena Zherebina to chiral separations, and D. Babusis for DMPK sample analysis data. We also thank Curtis E Moore from the Rheingold lab, UC San Diego, for assistance in the solving of crystal structures. These studies were in part supported by The Joint Science and Technology Office for Chemical and Biological Defense (JSTO-CBD) of the Defense Threat Reduction Agency (DTRA) under plan #CB10218. CDC core funding supported the work done by MKL at CDC

Disclaimer: Opinions, interpretations, conclusions, and recommendations are those of the authors and are not necessarily endorsed by the U.S. Army, U.S. Department of Health and Human Services, the Public Health Service, the Centers for Disease Control and Prevention, or the authors' affiliated institutions. Research was conducted under an IACUC approved protocol in compliance with the Animal Welfare Act, PHS Policy, and other Federal statutes and regulations relating to animals and experiments involving animals. The facility where this

research was conducted is accredited by the Association for Assessment and Accreditation of Laboratory Animal Care, International and adheres to principles stated in the Guide for the Care and Use of Laboratory Animals, National Research Council, 2011.

Abbreviations Used: EBOV, Ebola virus; EVD, Ebola virus disease; USAMRIID, United States Army Medical Research Institute of Infectious Diseases; SARS, severe acute respiratory syndrome; MERS, Middle East respiratory syndrome; BSL-4, Biosafety Level 4; HMVEC-TERT, human foreskin microvascular endothelial cells; RSV, respiratory syncytial virus; HEp-2, Human epithelial type 2 cell; Huh-7, Hepatocellular carcinoma cell; MT4, Human leukemia T-cell; Pol, polymerase; NTP, nucleoside triphosphate; POLRMT, mitochondrial RNA polymerase; SNI, single nucleotide incorporation; NMI, *N*-methyl imidazole; PNP, *para*-nitrophenol; PFP, pentafluorophenol; LG, leaving group; LogD, logarithm of distribution coefficient; Macro, human macrophage cells; NHP, nonhuman primate; IND, investigational new drug; SD, standard deviation; PBMC, peripheral blood mononuclear cell; IACUC, Institutional Animal Care and Use Committee.

REFERENCES

1. World Health Organization. *Ebola Situation Report - 10 June 2016.* http://apps.who.int/iris/bitstream/10665/208883/1/ebolasitrep_10Jun2016_eng.pdf?ua=1 (accessed July 22, 2016).
2. World Health Organization. *Ebola Data and Statistics – 11 May 2016*. http://apps.who.int/gho/data/view.ebola-sitrep.ebola-summary-20160511?lang=en (accessed July 22, 2016).

3. Vetter, P.; Fischer, W. A. II; Schibler, M.; Jacobs, M.; Baushc, D. G.; Kaiser, L. Ebola Virus Shedding and Transmission: Review of Current Evidence. *J. Infect. Dis.* **2016**, S1-S8.

4. Mate, S. E.; Kugelman, J. R.; Nyenswah, T. G.; Ladner, J. T.; Wiley, M. R.; Cordier-Lassalle, T.; Christie, A.; Schroth, G. P.; Gross, S. M.; Davies-Wayne, G. J.; Shinde, S. A.; Murugan, R.; Sieh, S. B.; Badio, M.; Fakoli, L.; Taweh, F.; de Wit, E.; van Doremalen, N.; Munster, V. J.; Pettitt, J.; Prieto, K.; Humrighouse, B. W.; Ströher, U.; DiClaro, J. W.; Hensley, L. E.; Schoepp, R. J.; Safronetz, D.; Fair, J.; Kuhn, J. H.; Blackley, D. J.; Laney, A. S.; Williams, D. E.; Lo, T.; Gasasira, A.; Nichol, S. T.; Formenty, P.; Kateh, F. N.; De Cock, K. M.; Bolay, F.; Sanchez-Lockhart, M.; Palacios, G. Molecular Evidence of Sexual Transmission of Ebola Virus. *N. Engl. J. Med.* **2015**, *373*, 2448-2454.

5. Kuhn, J. H. Filoviruses: A Compendium of 40 Years of Epidemiological, Clinical, and Laboratory Studies; Calisher, C. H. Eds; SpringWien: New York, 2008.

6. Rougeron, V.; Feldmann, H.; Grard, G.; Becker, S.; Leroy, E. M. Ebola and Marburg Haemorrhagic Fever. *J. Clin. Virol.* **2015**, *64*, 111-119.

7. Qiu, X.; Wong, G.; Audet, J.; Bello, A.; Fernando, L.; Alimonti, J. B.; Fausther-Bovendo, H.; Wei, H.; Aviles, J.; Hiatt, E.; Johnson, A.; Morton, J.; Swope, K.; Bohorov, O.; Bohorova, N.; Goodman, C.; Kim, D.; Pauly, M. H.; Velasco, J.; Pettitt, J.; Olinger, G. G.; Whaley, K.; Xu, B.; Strong, J. E.; Zeitlin, L.; Kobinger, G. P. Reversion af Advanced Ebola Virus Disease in Nonhuman Primates With ZMapp. *Nature* **2014**, *514*, 47-53.

8. Thi, E. P.; Mire, C. E.; Lee, A. C. H.; Geisbert, J. B.; Zhou, J. Z.; Agans, K. N.; Snead, N. M.; Deer, D. J.; Barnard, T. R.; Fenton, K. A.; MacLachlan, I.; Geisbert, T. W. Lipid

Nanoparticles siRNA Treatment of Ebola-Virus-Makona-Infected Nonhuman Primates. *Nature* **2015**, *521*, 362-365.

9. Tekmira Pharmaceuticals Corporation. *Tekmira Provides Update On TKM-Ebola-Guinea*. http://www.sec.gov/Archives/edgar/data/1447028/000117184315003522/newsrelease.htm (2015) (accessed July 22, 2016).
10. Iversen, P. L.; Warren, T. K.; Wells, J. B.; Garza, N. L.; Mourich, D. V.; Welch, L. S.; Panchal, R. G.; Bavari, S. Discovery and Early Development of AVI-7537 and AVI-7288 For the Treatment of Ebola Virus and Marburg Virus Infections. *Viruses* **2012**, *4*, 2806-2830.
11. Oestereich, L.; Lüdtke, A.; Wurr, S.; Rieger, T.; Muñoz-Fontela, C.; Günther, S. Successful Treatment of Advanced Ebola Virus Infection With T-705 (favipiravir) in a Small Animal Model. *Antiviral Res.* **2014**, *105*, 17-21.
12. Smither, S. J.; Eastaugh, L. S.; Steward, J. A.; Nelson, M.; Lenk, R. P.; Lever, M. S. Post-exposure Efficacy of Oral T-705 (Favipiravir) Against Inhalational Ebola Virus Infection in a Mouse Model. *Antiviral Res.* **2014**, *104*, 153-155.
13. Sissoko, D.; Folkesson, E.; Abdoul, M.;Beavogui, A. H.; Gunther, S.; Shepherd, S.; Danel, C.; Mentre, F.; Anglaret, X.; Malvy, D. Favipiravir in Patients With Ebola Virus Disease: Early Results of the JIKI Trial in Guinea, CROI Conference, Boston, MA, Feb 22–25, 2016. [Abstract 103-ALB]. *Conference on Retroviruses and Opportunistic Infections* Seattle, WA, 2015.
14. McMullan, L. K.; Flint, M.; Dyall, J.; Albariño, C.; Olinger, G. G.; Foster, S.; Sethna, P.; Hensley, L. E.; Nichol, S. T.; Lanier, E. R.; Spiropoulou, C. F. The Lipid Moiety of

Brincidofovir is Required For In Vitro Antiviral Activity Against Ebola Virus. *Antiviral Res.* **2016**, *125*, 71-78.

15. Warren, T. K.; Wells, J.; Panchal, R. G.; Stuthman, K. S.; Garza, N. L.; Van Tongeren, S. A.; Dong, L.; Retterer, C. J.; Eaton, B. P.; Pegoraro, G.; Honnold, S.; Bantia, S.; Kotian, P.; Chen, X.; Taubenheim, B. R.; Welch, L. S.; Minning, D. M.; Babu, Y. S.; Sheridan, W. P.; Bavari, S. Protection Against Filovirus Disease by a Novel Broad-Spectrum Nucleoside Analogue BCX4430. *Nature* **2014**, *508*, 402-405.
16. Henao-Restrepo, A. M.; Longini, I. M.; Egger, M.; Dean, N. E.; Edmunds, W. J.; Camacho, A.; Carroll, M. W.; Doumbia, M.; Draguez, B.; Duraffour, S.; Enwere, G.; Grais, R.; Gunther, S.; Hossmann, S.; Kondé, M. K.; Kone, S.; Kuisma, E.; Levine, M. M.; Mandal, S.; Norheim, G.; Riveros, X.; Soumah, A.; Trelle, S.; Vicari, A. S.; Watson, C. H.; Kéïta, S.; Kieny, M. P.; Røttingen, J.-A. Efficacy and Effectiveness of an rVSV-Vectored Vaccine Expressing Ebola, Surface Glycoprotein: Interim Results From the Guinea Ring Vaccination Cluster-Randomised Trial. *Lancet* **2015**, *386*, 857-866.
17. Warren, T. K.; Jordan, R.; Lo, M. K.; Ray, A. S.; Mackman, R. L.; Soloveva, V.; Siegel, D.; Perron, M.; Bannister, R.; Hui, H. C.; Larson, N.; Strickley, R.; Wells, J.; Stuthman, K. S.; Van Tongeren, S. A.; Garza, N. L.; Donnelly, G.; Shurtleff, A. C.; Retterer, C. J.; Gharaibeh, D.; Zamani, R.; Kenny, T.; Eaton, B. P.; Grimes, E.; Welch, L. S.; Gomba, L.; Wilhelmsen, C. L.; Nichols, D. K.; Nuss, J. E.; Nagle, E. R.; Kugelman, J. R.; Palacios, G.; Doerffler, E.; Neville, S.; Carra, E.; Clarke, M. O.; Zhang, L.; Lew, W.; Ross, B.; Wang, Q.; Chun, K.; Wolfe, L.; Babusis, D.; Park, Y.; Stray, K. M.; Trancheva, I.; Feng, J. Y.; Barauskas, O.; Xu, Y.; Wong, P.; Braun, M. R.; Flint, M.; McMullan, L. K.; Chen, S. S.; Fearns, R.; Swaminathan, S.; Mayers, D. L.; Spiropoulou, C. F.; Lee, W.

A.; Nichol, S. T.; Cihlar, T.; Bavari, S. Therapeutic Efficacy of The Small Molecule GS-5734 Against Ebola Virus in Rhesus Monkeys. *Nature* **2016**, *531*, 381-385.

18. Mehellou, Y.; Balzarini, J.; McGuigan, C. Aryloxy Phosphoramidate Triesters: A Technology For Delivering Monophosphorylated Nucleosides and Sugars Into Cells. *Chem. Med. Chem.* **2009**, *4*, 1779-1791.
19. Sofia, M. J.; Bao, D.; Chang, W.; Du, J.; Nagarathnam, D.; Rachakonda, S.; Reddy, P. G.; Ross, B. S.; Wang P.; Zhang, H.-R.; Bansal, S.; Espiritu, C.; Keilman, M.; Lam, A. M.; Micolochick Steuer, H. M.; Niu, C.; Otto, M. J.; Furman, P. A. Discovery of a β-D-2′-Deoxy-2′-α-Fluoro-2′-β-*C*-Methyluridine Nucleotide Prodrug (PSI-7977) For the Treatment of Hepatitis C Virus. *J. Med. Chem.* **2010**, *53*, 7202-7218.
20. Lee, A. W.; He, G.-X.; Eisenberg, E.; Cihlar, T.; Swaminathan, S.; Mulato, A.; Cundy, K. C. Selective Intracellular Activation of a Novel Prodrug of the Human Immunodeficiency Virus Reverse Transcriptase Inhibitor Tenofovir Leads to Preferential Distribution and Accumulation in Lymphatic Tissue. *Antimicrob. Agents Chemother.* **2005**, *49*, 1898-1906.
21. Murakami, E.; Niu, C.; Bao, H.; Micolochick Steuer, H. M.; Whitaker, T.; Nachman, T.; Sofia, M. A.; Wang, P.; Otto, M. J.; Furman, P. A. The Mechanism of Action of β-D-2′-Deoxy-2′-Fluoro-2′-*C*-Methylcytidine Involves a Second Metabolic Pathway Leading to β-D-2′-Deoxy-2′-Fluoro-2′-*C*-Methyluridine 5′-Triphosphate, A Potent Inhibitor of the Hepatitis C Virus RNA-Dependent RNA Polymerase. *Antimicrob. Agents Chemother.* **2008**, *52*, 458-464.

22. Cho, A.; Suanders, O. L.; Butler, T.; Zhang, L.; Xu, J.; Vela, J. E.; Feng, J. Y.; Ray, A. S.; Kim, C. U. Synthesis and Antiviral Activity of a Series of 1′-Substituted 4-Aza-7,9-Dideazaadenosine *C*-Nucleosides. *Bioorg. Med. Chem. Lett.* **2012**, *22*, 2705-2707.

23. Mackman, R. L.; Parrish, J. P.; Ray, A. S.; Theodore, D. A. Methods and Compounds For Treating Paramyxoviridae Virus Infections. U.S. Patent 2011045102 July, 22, 2011.

24. Patil, S. A.; Otter, P. B.; Klein, R. S. 4-Aza-7,9-Dideazaadenosine, A New Cytotoxic Synthetic *C*-Nucleoside Analogue of Adenosine. *Tetrahedron Lett.* **1994**, *35*, 5339-5342.

25. Lou, Z.; Chen, G.; Xie, Y. Cyanoribofuranoside Compound and its Preparing Method. Chinese Patent CN1137132C February, 4, 2004.

26. Yoshimura, Y.; Kano, F.; Miyazaki, S.; Ashida, N.; Sakata, S. Synthesis and Biological Evaluation of 1′-*C*-Cyano-Pyrimidine Nucleosides. *Nucleosides Nucleotides* **1996**, *15*, 305–324.

27. Kirschberg, T. A.; Mish, M.; Squires, N. H.; Zonte, S.; Aktoudianakis, E.; Metobo, S.; Butler, T.; Ju, X.; Cho, A.; Ray, A. S.; Kim, C. U. Synthesis of 1′-*C*-Cyano Pyrimidine Nucleosides and Characterization as HCV Polymerase Inhibitors. *Nucleosides, Nucleotides and Nucleic Acids* **2015**, *34*, 763-785.

28. Cho, A.; Zhang, L.; Xu, J.; Lee, R.; Butler, T.; Metobo, S.; Aktoudianakis, V.; Lew, W.; Ye, H.; Clarke, M.; Doerffler, E.; Byun, D.; Wang, T.; Babusis, D.; Carey, A. C.; Berman, P.; Sauer D.; Zhong, W.; Rossi, S.; Fenaux, M.; McHutchison, J. G.; Perry, J.; Feng, J.; Ray, A. S.; Kim, C. U. Discovery of the First *C*-nucleoside HCV Polymerase Inhibitor (GS-6620) With Demonstrated Antiviral Response in HCV Infected Patients. *J. Med. Chem.* **2014**, *57*, 1812-1825.

29. (a) Smith, J. T; Elkin, J. T.; Monty Reichert, W. Directed Cell Migration on Fibronectin Gradients: Effect of Gradient Slope. *Exp. Cell Res.* **2006**, *312*, 2424-2432. (b) Zhao, L.; Kroenke, C. D.; Song, J.; Piwnica-Worms, D.; Ackerman, J. J. H.; Neil, J. J. Intracellular Water Specific MR of Microbead-Adherent Cells: The HeLa Cell Intracellular Water Exchange Lifetime. *NMR Biomed.* **2008**, *21*, 159-164.

30. Clarke, M. O.; Mackman, R.; Byun, D.; Hui, H.; Barauskas, O.; Birkus, G.; Chun, B.-K.; Doerffler, E.; Feng, J.; Karki, K.; Lee, G.; Perron, M.; Siegel, D.; Swaminathan, S.; Lee, W. Discovery of β-D-2′-α-Fluoro-4′-α-Cyano-5-Aza-7,9-Dideaza Adenosine as a Potent Nucleoside Inhibitor of Respiratory Syncytial Virus With Excellent Selectivity Over Mitochondrial RNA and DNA Polymerases. *Bioorg. Med. Chem. Lett.* **2015**, *25*, 2484-2487.

31. Feng, J.; Xu, Y.; Barauskas, O.; Perry, J. K.; Ahmadyar, S.; Stepan, G.; Yu, H.; Babusis, D.; Park, Y.; McCutcheon, K.; Perron, M.; Schultz, B. E.; Sakowicz, R.; Ray, A. S. Role of Mitochondrial RNA Polymerase in the Toxicity of Nucleotide Inhibitors of Hepatitis C Virus. *Antimicrob. Agents Chemother.* **2016**, *60*, 806-817.

32. (a) Müller, R.; Poch, O.; Delarue, M.; Bishop, D. H. L.; Bouloy, M. Rift Valley Fever Virus L Segment: Correction of the Sequence and Possible Functional Role of Newly Identified Regions Conserved in RNA-Dependent Polymerases. *J. Gen. Virol.* **1994**, *75*, 1345-1352. (b) Huang, H.; Chopra, R.; Verdine, G. L.; Harrison, S. C. Structure of a Covalently Trapped Catalytic Complex of HIV-1 Reverse Transcriptase: Implications For Drug Resistance. *Science* **1998**, *282*, 1669-1675. (c) Appleby, T. C.; Perry, J. K.; Murakami, E.; Barauskas, O.; Feng, J.; Cho, A.; Fox, D.; Wetmore, D. R.; McGrath, M.

E.; Ray, A. S.; Sofia, M. J.; Swaminathan, S.; Edwards, T. E. Structural Basis For RNA Replication by the Hepatitis C Virus Polymerase. *Science* **2015**, *347*, 771-775.

33. For active site models of other filovirus polymerases see supplementary information.
34. Feng, J. Y.; Cheng, G.; Perry, J.; Barauskus, O.; Xu, Y.; Fenaux, M.; Eng, S.; Tirunagari, N.; Peng, B.; Yu, M.; Tian, Y.; Lee, Y.-J.; Stepan, G.; Lagpacan, L. L.; Jin, D.; Hung, M.; Ku, K. S.; Han, B.; Kitrinos, K.; Perron, M.; Birkus, G.; Wong, K. A.; Zhong, W.; Kim, C. U.; Carey, A.; Cho, A.; Ray, A. S. Inhibition of Hepatitis C Virus Replication by GS-6620, a Potent *C*-Nucleoside Monophosphate Prodrug. *Antimicrob. Agents Chemother.* **2014**, *58*, 1930-1942.
35. Butler, T.; Cho, A.; Kim, C. U.; Saunders, O. L.; Zhang, L. 1′-Substituted Carba-Nucleoside Analogues For Antiviral Treatment. U.S. Patent 2009041447 April, 22, 2009.
36. Butler, T.; Cho, A.; Graetz, B. R.; Kim, C. U.; Metobo, S. E.; Saunders, O. L.; Waltman, A. W.; Xu, J.; Zhang, L. Processes and Intermediates For the Preparation of 1′-Substituted Carba-Nucleoside Analogues. U.S. Patent 20100459508 September, 20, 2010.
37. Metobo, S. E.; Xu, J.; Saunders, O. L.; Butler, T.; Aktoudianakis, E.; Cho, A.; Kim, C. U. Practical Synthesis of 1′-Substituted Tubercidin *C*-Nucleoside Analogs. *Tetrahedron Lett.* **2012**, *53*, 484-486.
38. Axt, S. D.; Badalov, P. R.; Brak, K.; Campagna, S.; Chtchemelinine, A.; Chun, B. K.; Clarke, M. O. H.; Doerffler, E.; Frick, M. M.; Gao, D.; Heumann, L. V.; Hoang, B.; Hui, H. C.; Jordan R.; Lew, W.; Mackman, R. L.; Milburn, R. R.; Neville, S. T.; Parrish, J. P.; Ray, A. S.; Ross, B.; Rueden, E.; Scott, R. W.; Siegel, D.; Stevens, A. C.; Tadeus, C.;

Vieira, T.; Waltman, A. W.; Wang, X.; Whitcomb, M. C.; Wolfe, L.; Yu, C.-Y. Methods For Treating Filoviridae Virus Infections. U.S. Patent 2015017934, October 29, 2015.

39. Krasovskiy, A.; Knochel, P. A LiCl-Mediated Br/Mg Exchange Reaction For the Preparation of Functionalized Aryl- and Heteroarylmagnesium Compounds From Organic Bromides. *Angew. Chem. Int. Ed*. **2004**, *43*, 3333–3336.
40. For a separate account describing the crystallization induced resolution of *p*-nitrophenolate 2-ethylbutyl-L-alaninate phosphoramidate see: Klasson, B.; Eneroth, A.; Nilson, M.; Pinho, P.; Samuelsson, B.; Sund, C. HCV Polymerase Inhibitors. European Patent IB2012056994 December 5, 2012. The conditions in this manuscript were identified independently/concurrently with this report.
41. Bahar, F. G.; Ohura, K.; Ogihara, T.; Imai, T. Species Difference of Esterase Expression and Hydrolase Activity in Plasma. *J. Pharm. Sci.* **2012**, *101*, 3979-3988.
42. Jacobs, M.; Rodger, A.; Bell, D. D.; Bhagani, S.; Cropley, I.; Filipe, A.; Gifford, R. J.; Hopkins, S.; Hughes, J.; Jabeen, F.; Johannessen, I.; Karageorgopoulos, D.; Lackenby, A.; Lester, R.; Liu, R. S. N.; MacConnachie, A.; Mahungu, T.; Martin, D.; Marshall, N.; Mepham, S.; Orton, R.; Pamarini, M.; Patel, M.; Perry, C.; Peters, S. E.; Porter, D.; Ritchie, D.; Ritchie, N. D.; Seaton, R. A.; Sreenu, V. B.; Templeton, K.; Warren, S.; Wilkie, G. S.; Zambon, M.; Gopal, R.; Thomson, E. C. Late Ebola Virus Relapse Causing Meningoencephalitis: A Case Report. *Lancet*, **2016**, *388*, 498-503.
43. Schnirring, L. Center For Infectious Disease Research and Policy. Youngest Ebola Survivor Leaves Guinea Hospital. http://www.cidrap.umn.edu/news-perspective/2015/11/youngest-ebola-survivor-leaves-guinea-hospital, November 30, 2015 (accessed July 22, 2016).

44. National Institues of Health. PREVAIL Treatment Trial For Men With Persistent Ebola Viral RNA in Semen Opens in Liberia. https://www.nih.gov/news-events/news-releases/prevail-treatment-trial-men-persistent-ebola-viral-rna-semen-opens-liberia, July 5, 2016. (accessed, July, 22, 2016).

TABLE OF CONTENT GRAPHIC

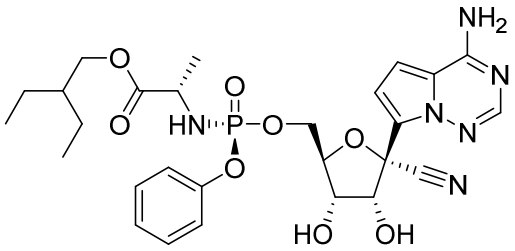

EBOV (Macrophage)

EC_{50} = 86 nM